CONTINUUM RELAXATION OF INTERACTING STEPS ON CRYSTAL SURFACES IN 2+1 DIMENSIONS

DIONISIOS MARGETIS* AND ROBERT V. KOHN†

Abstract. We study the relaxation of crystal surfaces in 2+1 dimensions via the motion of interacting atomic steps. The goal is the rigorous derivation of the continuum limit. The starting point is a discrete scheme from the Burton, Cabrera and Frank ("BCF") model, which accounts for diffusion of point defects ("adatoms") on terraces and attachment-detachment of atoms at step edges. It is shown that the macroscopic adatom current involves a tensor mobility, which describes different fluxes in directions parallel and transverse to step edges, although the physics of each terrace is assumed isotropic. When the steps are everywhere parallel (straight or circular) the tensor character of the mobility is unimportant; in the general (2+1)-dimensional setting, however, it is crucial. Our methods consist of: (i) the solution of the diffusion equation for adatoms via the separation of local space variables into "fast" and "slow"; and (ii) the treatment of the step chemical potential for a wide class of step energies and repulsive interactions. Previous works using similar methods were mainly restricted to (1+1)-dimensional or axisymmetric geometries and entirely missed the tensor character of the mobility. The continuum limit of the step flow yields a fourth-order partial differential equation (PDE) for the surface height profile.

Key words. crystal surface, epitaxial growth, morphological evolution, Burton-Cabrera-Frank (BCF) model, Ehrlich-Schwoebel barrier, entropic interactions, elastic dipole interactions, step chemical potential, continuum limit, surface mobility

AMS subject classifications. 35Q99, 35R35, 74A50

1. Introduction.

Small devices that advance communications technology rely on the synthesis of surface structures on crystalline materials. The derivation and application of evolution laws for surface morphologies remain actively pursued problems involving various length and time scales, from the atomistic to the continuum.

The dynamics and kinetics of crystal surfaces depend on the temperature, T ([23]). Below the surface orientation dependent roughening transition temperature, $T_{\rm R}$, crystal surfaces evolve via the motion of distinct steps with atomic height and nanoscale terraces, and may develop macroscopic, flat regions ("facets"). For $T > T_{\rm R}$ steps are created spontaneously, terraces are not identified, and facets shrink to extinction.

The step motion is affected by: (i) the step kinetics, which incorporate atom diffusion and attachment-detachment at step edges; (ii) the step energetics, which include the tendency of closed steps to reduce their length via motion driven by curvature, as well as interactions between steps that extend from nearest to far neighbors; and (iii) the presence of material deposition from above. In the absence of deposition, crystal surfaces tend to relax to equilibrium and become flat under the influence of step energetics and kinetics. In this article, we address considerations (i) and (ii) for surface relaxation, including the effects of beyond-nearest-neighbor step interactions.

There are two basic theoretical approaches to crystal surface morphological evolution. One approach follows the motion of individual steps on the basis of the Burton, Cabrera and Frank [3] ("BCF") model, accounting for diffusion of point defects ("adatoms") on terraces and atom attachment-detachment at step edges; cf. Sec. 2.1 for a review. In this context surface morphologies below $T_{\rm R}$ are described via numerical solutions ("kinetic simulations") of coupled differential equations for step po-

*Department of Mathematics, Massachusetts Institute of Technology, 77 Massachusetts Avenue, Cambridge, MA 02139 (dio@math.mit.edu).

†Courant Institute, New York University, 251 Mercer Street, New York, NY 10012 (kohn@cims.nyu.edu). This work was partially supported by NSF through grant DMS 0313744.

sitions. Kinetic simulations provide detailed information ([21, 22]) for morphologies where steps are everywhere parallel. Because of the large number of variables involved, however, this approach appears limited in making predictions for more general cases.

Another approach is based on continuum thermodynamics and mass conservation, using continuum evolution equations such as partial differential equations (PDEs), and variational principles. Continuum theories are amenable to simple predictions and are known to describe adequately surface morphologies above $T_{\rm R}$. Over 40 years ago, the morphological relaxation by surface diffusion of corrugated surfaces above $T_{\rm R}$ was formulated via a continuum surface free energy that is an analytic function of the surface orientation ([19, 33, 34]). Essential in this formulation is the chemical potential ([19]), which is proportional to surface curvature and has a gradient proportional to surface current. The continuum approach is questionable below $T_{\rm R}$, where the surface free energy is not an analytic function of surface orientation ([17]).

The relation of the two theoretical approaches for temperatures below $T_{\rm R}$ has received only modest attention ([20, 37, 32]). Continuum descriptions of surface diffusion in close correspondence to BCF-type models have been derived for steps that are everywhere parallel such as straight steps in 1+1 dimensions and circular steps in 2+1 dimensions with axisymmetry; cf. Sec. 2.2 for a review of the step motion equations for axisymmetric profiles. In the case with parallel steps the surface current is normal to step edges and is related to the gradient of the chemical potential via a scalar, slope-dependent mobility. Continuum evolution laws in 2+1 dimensions for steps of arbitrary shape have been speculated ([41, 30]) by direct comparisons with models in 1+1 dimensions and, thus, make use of a scalar surface mobility even for isotropic diffusion across terraces.

In this article we show that this analogy with one-dimensional step flow models is inadequate to describe surface relaxation with step edges that are not everywhere parallel, further developing ideas outlined by one of us recently in a letter ([29]). Our analysis relies on the assumption that the width of vicinal terraces, a microscopic length, is small compared to: (i) the macroscopic length over which the step density varies; (ii) the step radius of curvature; and (iii) the length over which the step curvature varies. Throughout this article we refer to step trains that satisfy (i)–(iii) as "slowly varying". The terrace width is considered comparable to or larger than the step height so that in the continuum limit the step density properly approaches the surface slope. We focus on geometries with descending steps and vicinal terraces surrounding a top terrace (surface peak) and do not address step motion near a bottom terrace (surface valley). These restrictions enable mathematical approximations while keeping intact the essential physics of the BCF model.

In particular, we show that for isotropic terrace diffusion (in the absence of material deposition from above) the continuum-scale surface current, $\mathbf{J}$, is related to the gradient of the step chemical potential, μ, which is defined as the change in the step energy by addition or removal of an atom at a step edge, via a tensor mobility,

$$\mathbf{J} = \mathcal{M}_1(|\nabla h|)\,\nabla_\perp \mu + \mathcal{M}_2(|\nabla h|)\,\nabla_\parallel \mu\,. \tag{1.1}$$

Here, h is the coarse-grained surface height profile, $\mathcal{M}_1$ and $\mathcal{M}_2$ are proportional to matrix elements of the mobility tensor, $\mathbf{M}$, and $\nabla_\perp$ and $\nabla_\parallel$ denote gradients normal and parallel to step edges; cf. (4.8)–(4.10) and (4.21). The chemical potential μ is given by (4.22), and the height h evolves by mass conservation, (4.34). The first term in (1.1) is the transverse current, which is a natural generalization of the radial case (with circular steps) ([30]). The second term in (1.1) is the longitudinal current, in

principle nonzero for non-parallel steps, which is driven by mass conservation through terrace diffusion. Equation (1.1) describes the macroscopic, anisotropic joint effect on $\mathbf{J}$ of diffusion-induced adatom fluxes transverse and parallel to step edges, which is absent from previous treatments ([41, 30]) of crystal surface morphological relaxation.

Anisotropies of surface currents have been formulated within different models, such as those accounting for atom diffusion along step edges ([23, 9]) and step meandering ([7]), where the underlying, microscopic physics of adatom diffusion is manifestly anisotropic. By contradistinction to these cases, the anisotropy in (1.1) originates from the direct coarse graining of a physical model with isotropic diffusion on each terrace. Our analysis demonstrates that (1.1) is a consequence of the form of boundary conditions imposed on adatom fluxes at step edges bounding each terrace.

By adopting the view that BCF-type models offer a discrete scheme for macroscopic evolution equations, we seek such an equation for the surface height profile, h, in 2+1 dimensions for surface relaxation. For this purpose we combine the surface current (1.1) with continuum laws for μ and $\mathbf{J}$; cf. (4.22) and (4.34). As a result we derive a nonlinear, fourth-order PDE for h when steps interact via nearest-neighbor repulsions, describing the combined effect of step energetics and kinetics, and surface topography; cf. (4.39). Possible connections of this PDE to experimental observations ([24, 12]) of decaying surface profiles, although incomplete at the moment ([29]), can be useful for predicting lifetimes and other properties of surface structures.

The considerations discussed above, which focus on surface relaxation via nearest-neighbor step interactions, enable simplicity of the exposition with emphasis on the (2+1)-dimensional geometry, but also form a basis for the treatment of more general cases. Such cases include elastic effects ([8]), by which steps interact beyond nearest neighbors. In this article we extend our analysis to include these effects in the macroscopic laws. We show that in the absence of bulk stress ([28, 25]), when steps interact via short-range, entropic repulsions and as elastic dipoles with repulsive forces extending beyond their closest neighbors, the continuum evolution laws in 2+1 dimensions remain local. This result, previously known for (1+1)-dimensional geometries ([42]), justifies the use of nearest-neighbor step interactions in (2+1)-dimensional models. Furthermore, we discuss more generally conditions on the step interactions that leave intact the local character of the continuum. The more demanding case with bulk stress, when step interactions give rise to non-local evolution laws, is left for future work.

In this article we do not address the numerical treatment of the derived evolution laws. One reason is the present lack of suitable boundary conditions at facet edges, which are free boundaries where continuum solutions develop singularities. Another reason is our lack of understanding of the behavior of continuum solutions that are relevant to realistic, experimental situations. Both of these topics, boundary conditions and connections to experiments, are subjects of work in progress.

It is beyond the scope of this article to offer an exhaustive list of works on crystal surface morphological evolution. There is vast literature on the derivation of continuum laws, either from step flow models or from more phenomenological, continuum thermodynamics principles. Reviews that explore this body of work can be found in [13, 32, 37]. Within the step flow approach and in the absence of deposition, early works ([35, 38, 36]) focus on the continuum limit of BCF-type models in 1+1 dimensions for interacting steps. Derivations of PDEs in 1+1 and 2+1 dimensions for various kinetic laws with non-interacting steps are outlined in [9], where the macroscopic effect of longitudinal (parallel to step edges) adatom fluxes induced by terrace diffusion is apparently absent. Extensions to include elastic effects are described in [48, 49]

on the basis of discrete models formulated in [8, 47]. The derivation from step flow equations of a PDE for axisymmetric profiles is described in [30]; this work is reviewed in Sec. 2.2 because it is used here as a guide for treating (2+1)-dimensional settings.

Within the continuum thermodynamics approach, progress has been hindered by the consideration of crystal facets, at the edges of which continuum solutions are singular and the motion of extremal steps must be considered ([5, 21, 30, 15]). Facet evolution is first treated in [43, 18] as a free-boundary problem via a continuum surface free energy, G, that is a non-analytic function of the surface orientation ([17]). The difficulty of the facet is circumvented via a related, variational formulation in [42, 41, 6]. An ingredient of this approach is a scalar surface mobility, which for 2+1 dimensions is speculated ([41, 6]) by direct analogy with step models in 1+1 dimensions ([3, 38, 36]). The same free energy and mobility are invoked in [30], where macroscopic evolution laws in 2+1 dimensions are formulated via differentiations of G in surface regions outside the facet. Studies ([42, 48]) of step interactions in 1+1 dimensions have shown that the evolution laws are local in the absence of bulk stress, when crystalline steps interact as elastic dipoles ([25]) and via short-range, entropic repulsions ([23]).

Our article addresses only surface relaxation by accounting for the motion of steps, thus focusing on a kinetic regime where evolution occurs via a decreasing surface free energy as expected by thermodynamics. The entirely different kinetic regime with material deposition from above in 2+1 dimensions is treated elsewhere ([31]).

The article is organized as follows. In Sec. 2 we review the BCF framework: In Sec. 2.1 we outline the basic ingredients; and in Sec. 2.2 we revisit the equations of motion and continuum limit for circular, concentric steps. In Sec. 3 we formulate the discrete equations of motion for the relaxation of a slowly varying step train near a top terrace in 2+1 dimensions, allowing for the presence of the Ehrlich-Schwoebel ("ES") barrier [10, 40]: In Sec. 3.1 we determine approximately the adatom density on each terrace by separating the local step coordinates into "fast" and "slow"; in Sec. 3.2 we study the discrete step chemical potential for pairwise step interactions; and in Sec. 3.3 we describe the step velocity law. In Sec. 4 we consider the continuum limit of the discrete step flow equations for surface relaxation: In Sec. 4.1 we derive the surface current and mobility coefficients of (1.1) from the boundary conditions for the adatom density at step edges; in Sec. 4.2 we derive the continuum-scale step chemical potential for nearest-neighbor, dipole and entropic step repulsions; in Sec. 4.3 we derive the familiar statement of mass conservation for atoms; in Sec. 4.4 we derive an evolution equation for the surface height profile; and in Sec. 4.5 we sketch alternative derivations by using a weak formulation and a continuum surface free energy. In Sec. 5 we consider extensions of the continuum theory: In Sec. 5.1 we discuss more general step-step interactions; and in Sec. 5.2 we include orientation-dependent step energies. In Sec. 6 we discuss limitations of our approach and related, open problems. In the appendices we provide some proofs and derivations that are needed in the main text.

2. Background. In this section we give the background needed for developing a (2+1)-dimensional continuum theory. First, we outline the basic elements of the BCF approach and their interrelations. Second, we illustrate the equations of coupled step motion and their continuum limit without material deposition for a train of circular, interacting steps, where the (source-free) diffusion equation for adatoms on terraces is exactly solvable and the adatom density is obtained in simple closed form.

2.1. BCF approach. In the spirit of the seminal BCF theory ([3]), we adopt the view that step edges are smooth curves whose motion is determined by attachment and detachment of atoms via conservation of mass; so, the steps move with a velocity

proportional to the sum of normal adatom fluxes incident on the step edge from adjacent terraces. The adatom density solves the diffusion equation on each terrace with suitable boundary conditions for atom attachment-detachment at the step edges. A variety of such boundary conditions have been considered in the literature ([21, 9, 16, 27, 45, 4, 2]). Here, we focus on the simplest class of step models that is rich enough to include the effects of: (i) step edge curvature; (ii) pairwise step interactions; and (iii) finite, kinetic rates of atom attachment-detachment at step edges.

We proceed to offer a more quantitative description of the step motion. We consider the diffusion of adatoms across terraces and the attachment-detachment of atoms at step edges as the major kinetic processes. Three ingredients of this approach are: (i) the adatom density, $C^{\rm ter}$, and current, $\mathbf{J}^{\rm ter}$, on each terrace, where $C^{\rm ter}$ satisfies the diffusion equation; (ii) the step chemical potential, $\mu^{\rm st}$, which accounts for the effect of step energy on motion; and (iii) the step velocity, v.

First, we introduce $C^{\rm ter}$. It solves

$$\partial_t C^{\rm ter} = \nabla \cdot (\mathbf{D}_{\rm s} \nabla C^{\rm ter}) + F \qquad \mathbf{r} \text{ on terrace}, \tag{2.1}$$

where $\partial_t = \partial/\partial t$ and $\mathbf{D}_{\rm s}$ is the terrace diffusivity, in principle a tensor function of the position vector $\mathbf{r}$. In (2.1) we neglect atom desorption on the terrace but allow for the possibility of material deposition from above with flux F. The focus of the present paper is surface relaxation; so, in Sec. 2.2 and beyond we set $F = 0$. We assume isotropic and homogeneous terrace diffusion throughout this article, and thus take $\mathbf{D_s}$ to be a scalar constant, $\mathbf{D}_{\rm s} = D_{\rm s}$. In addition, we apply the "quasi-steady approximation", by which adatoms diffuse faster than steps move, so that $\partial_t C^{\rm ter} \approx 0$ and time dependence enters implicitly through the moving boundary. The adatom current on a terrace is defined by $\mathbf{J}^{\rm ter} = -D_{\rm s} \nabla C^{\rm ter}$ where $\nabla \cdot \mathbf{J}^{\rm ter} = F$.

Second, we describe boundary conditions for solving (2.1). Atom attachment and detachment at a step edge are described by the kinetic law

$$f_\pm = k_\pm \, (C_\pm - C^{\rm eq}), \qquad f_\pm = \hat{\mathbf{n}}_\pm \cdot \mathbf{J}^{\rm ter}_\pm, \tag{2.2}$$

where $f_\pm$ is the normal adatom flux from the upper $(+)$ or lower $(-)$ terrace towards the step edge, $C^{\rm ter}_\pm$ and $\mathbf{J}^{\rm ter}_\pm$ are the adatom density and current at the edge, $k_\pm$ is the attachment-detachment rate coefficient, in principle different for an up- and down-step edge in order to account for the ES barrier ([10, 40]), $C^{\rm eq}$ is the equilibrium atom density at the edge, and $\hat{\mathbf{n}}_\pm$ is the unit vector normal to the edge pointing outwards the upper $(+)$ or lower $(-)$ terrace. In (2.2) we neglect $vC_\pm$ where v is the step velocity. This term is necessary for mass conservation but is small in most epitaxial phenomena; its neglect is consistent with the imposed quasi-steady approximation.

Next, we introduce the step chemical potential, $\mu^{\rm st}$, which involves step energies and relates $\mathbf{J}^{\rm ter}$ with the step edge positions. Following [23, 21] we use

$$C^{\rm eq} = C_{\rm s} \, \exp \frac{\mu^{\rm st}}{k_{\rm B} T} \sim C_{\rm s} \left(1 + \frac{\mu^{\rm st}}{k_{\rm B} T} \right), \tag{2.3}$$

where $C_{\rm s}$ is the equilibrium atom density near a straight and isolated step edge, $k_{\rm B}$ is Boltzmann's constant, and $|\mu^{\rm st}| \ll k_{\rm B} T$ ([46]). In general, $\mu^{\rm st}$ depends on the step edge curvature and positions; cf. Sec. 2.2 for circular steps. For non-interacting steps $\mu^{\rm st}$ is proportional to the step curvature according to the Gibbs-Thomson formula ([39, 21]). The adatom density, $C^{\rm ter}$, can be found as a function of the step chemical potential at the step boundaries through solving (2.1) with (2.2) and (2.3).

Mass conservation dictates that the velocity, v, by which a step advances be

$$v = \frac{\Omega}{a}\,(f_+ + f_-), \tag{2.4}$$

where Ω is the atomic volume and a is the step height, neglecting atom diffusion along the step edge ([23, 4, 9, 2]). In the next subsection we illustrate the step motion laws for the relaxation ($F = 0$) of axisymmetric crystal shapes.

2.2. Review of radial case for surface relaxation. We next describe the step motion and its continuum limit for circular steps and zero deposition flux ($F = 0$) by following [21] and [30], in order to guide the analysis of Secs. 3, 4. The geometry consists of concentric circular, descending steps numbered $i = 1, 2, \dots N$ with radii $r_i(t)$; the region $r_i < r < r_{i+1}$ is the ith terrace, a circular annulus, r is the polar distance and $r_0 \equiv 0$ for the top terrace ([30]).

2.2.1. Discrete step flow. We now present the rotationally symmetric step flow equations of the BCF approach by analogy with (2.1)–(2.4). The adatom current, $\mathbf{J}_i = -D_{\rm s}\nabla C_i$, on the ith terrace is normal to the step edges, in the radial direction, with component $J_i(r,t) = -D_{\rm s}\partial_r C_i$ where $C_i(r,t)$ is the adatom density.

First, we determine C_i and J_i in terms of the step chemical potential at the bounding step edges. By (2.1) C_i satisfies the one-dimensional (1D) equation

$$\frac{1}{r}\frac{\partial}{\partial r} r \frac{\partial C_i}{\partial r} = 0 \qquad r_i < r < r_{i+1}. \tag{2.5}$$

This equation is solved by $C_i(r,t) = A_i(t)\ln(r/r_i) + B_i(t)$ yielding $J_i(r,t) = -D_{\rm s}A_i(t)/r$, where $A_i(t)$ and $B_i(t)$ are determined by imposing (2.2) in the form

$$-J_i(r_i,t) = k_{\rm u}\,(C_i - C_i^{\rm eq}) \quad r = r_i, \quad J_i(r_{i+1},t) = k_{\rm d}\,(C_i - C_{i+1}^{\rm eq}) \quad r = r_{i+1}, \tag{2.6}$$

where $k_{\rm u}$ and $k_{\rm d}$ are kinetic rates for attachment-detachment from a terrace to an up- and down-step edge, respectively; $k_{\rm d} < k_{\rm u}$ for a positive ES barrier ([10, 40]). Hence,

$$J_i(r,t) = -\frac{D_{\rm s}C_{\rm s}}{k_{\rm B}T}\,\frac{\mu_{i+1} - \mu_i}{\ln(r_{i+1}/r_i) + D_{\rm s}[(k_{\rm u}r_i)^{-1} + (k_{\rm d}r_{i+1})^{-1}]}\,\frac{1}{r}, \tag{2.7}$$

where, by invoking (2.3), $\mu_i = \mu^{\rm st}$ is the chemical potential at the ith step edge.

Second, we describe μ_i as a function of the step edge radii. By the Gibbs-Thomson formula ([21, 30]), μ_i is proportional to the step edge curvature, $1/r_i$, in the absence of step interactions. With inclusion of step interactions ([21, 30]), μ_i is given by

$$\mu_i = \frac{\Omega}{a}\left[\frac{\gamma}{r_i} + \frac{1}{r_i}\,\partial_{r_i}(r_i U_i^{\rm int})\right], \tag{2.8}$$

where γ is the step line tension (energy/length) and $U_i^{\rm int}$ is the interaction energy per unit length. For nearest-neighbor, dipole and entropic step repulsions, $U_i^{\rm int}$ is ([21, 30])

$$U_i^{\rm int} = g[V(r_i, r_{i+1}) + V(r_i, r_{i-1})], \quad V(r,r') = \frac{1}{3}\,\frac{2r'}{r+r'}\left(\frac{a}{r-r'}\right)^2, \tag{2.9}$$

where g is the interaction strength (energy/length) and $g > 0$. Because $V(r,r')$ describes the interaction energy per unit length of a step at position r with the entire

step at r', V is not symmetric with (r, r'); cf. (2.9) and (3.21). Equations (2.8) and (2.9) yield μ_i as a function of r_i and $r_{i\pm1}$; $\mu_i = O[(r_{i+1} - r_i)^{-3}]$ as $r_{i+1} \to r_i$.

Next, we describe the velocity, $v_i = dr_i/dt$, of the ith step edge, which is determined as a function of r_i, $r_{i\pm1}$ and $r_{i\pm2}$ by applying (2.4),

$$v_i = \frac{\Omega}{a}[J_{i-1}(r_i, t) - J_i(r_i, t)], \tag{2.10}$$

along with (2.7)–(2.9). Equations (2.7)–(2.10) result in coupled differential equations for $r_i(t)$, which have been solved numerically for an initial conical shape ([21, 15]).

2.2.2. Continuum limit. By interpreting (2.7)–(2.10) as a discrete scheme for solving an evolution equation in continuous variables, the polar distance r and time t, we review the derivation of such a continuum equation for the coarse-grained height profile, $h(r, t)$ ([30]). In the continuum limit $r_i \equiv r$, $a/\lambda \to 0$ where λ is the macroscopic length over which the step density varies, $r_i \geq O(\lambda)$, and the terrace width, $\delta r_i = r_{i+1} - r_i$, approaches $a/|\partial_r h|$ where $\partial_r h = O(1) < 0$. The microscopic length δr_i is considered sufficiently smaller than: (i) the length λ, which is estimated by the mean value of $|\partial_r h/\partial_r^2 h|$ for surface regions outside the facet; and (ii) the step radius, r_i.

First, we derive a formula for the continuum-scale surface current, which is identified here with $J_i(r_i, t)$, the adatom current at the ith edge of the ith terrace, for definiteness. By (2.7) in the limit $a/r_i \to 0$ with $r_{i+1} \sim r_i - a/\partial_r h|_{r=r_i}$ we obtain ([30])

$$J_i(r_i, t) \to J(r, t) = -\frac{D_{\rm s} C_{\rm s}}{k_{\rm B} T} \frac{1}{1 + q\,|\partial_r h|}\, \partial_r \mu, \tag{2.11}$$

where $\mu(r, t)$ is the continuum step chemical potential via $\mu_{i+1} - \mu_i \sim \delta r_i\, \partial_r \mu$, and

$$q = \frac{2D_{\rm s}}{ka}, \quad k = 2\left(\frac{1}{k_{\rm u}} + \frac{1}{k_{\rm d}}\right)^{-1}. \tag{2.12}$$

The factor 2 is included so that $k \equiv k_{\rm u} = k_{\rm d}$ in the absence of the ES barrier.

Second, we find a formula for $\mu(r, t)$ in terms of the slope profile, $\partial_r h = -m$ where $m > 0$, by (2.8) and (2.9). We define the discrete step density, $m_i \equiv a/(r_{i+1} - r_i)$, of the ith step, by which $m_{i-1} = a/(r_i - r_{i-1})$. In the continuum limit m_i approaches the positive surface slope, $m_i \to m = |\partial_r h|\big|_{r=r_i}$, and m_{i-1} is properly expanded in Taylor series to yield ([30])

$$m_{i-1} \sim m_i - (a/m_i)(\partial_r m)|_{r=r_i}. \tag{2.13}$$

By carrying out the differentiations in (2.8) and invoking (2.13) we obtain ([30])

$$\mu(r, t) = \Omega g_1\, r^{-1} + \Omega\, g_3\, r^{-1}\, \partial_r[r(\partial_r h)^2], \tag{2.14}$$

where

$$g_1 = \frac{\gamma}{a}, \quad g_3 = \frac{g}{a}. \tag{2.15}$$

Equations (2.14) and (2.15) can also be derived by considering the surface free energy per projected area of the basal plane of Sec. 4.5; in particular, cf. (4.49).

Third, we derive the continuum mass conservation statement from the step velocity law (2.10). Because each terrace is a level set of the height, $(d/dt)h(r_i, t) =$

0, we deduce that $dr_i/dt \to \partial_t h/|\partial_r h|$. By solving (2.5) we find $r_i J_{i-1}(r_i,t) = r_{i-1}J_{i-1}(r_{i-1},t)$. Thus, with $r_iJ_i(r_i,t) - r_{i-1}J_{i-1}(r_{i-1},t) \sim \delta r_i \partial_r(rJ)$, (2.10) becomes

$$\partial_t h = -\Omega\, r^{-1}\partial_r(rJ). \tag{2.16}$$

Equations (2.11)–(2.16) yield a fourth-order PDE for the height profile ([30]),

$$B^{-1}\partial_t h = -r^{-1}\partial_r\left(\frac{r^{-1}}{1+q|\partial_r h|}\right) + \frac{g_3}{g_1}r^{-1}\partial_r\left[\frac{r}{1+q|\partial_r h|}\partial_r(r^{-1}\partial_r[r(\partial_r h)^2])\right], \tag{2.17}$$

where r is restricted to the region outside the facet, and B is the material parameter

$$B = \frac{\Omega^2\, g_1\, C_{\rm s}\, D_{\rm s}}{k_{\rm B}T}. \tag{2.18}$$

In Secs. 3, 4 the preceding calculations are extended to 2+1 dimensions. The necessary formulation and approximations for the discrete step flow are developed in the next section.

3. Slowly varying step train in 2+1 dimensions. In this section we formulate the equations of step motion with inclusion of the ES barrier ([10, 40]), in correspondence with the radial case, Sec. 2.2.1. First, we describe the step train in local, non-dimensional coordinates (η, σ), where η identifies individual steps and σ gives the position along a step edge. These variables are used for later convenience since solutions of the adatom diffusion equation on each terrace are found to depend explicitly on the distance from neighboring steps through η. Second, for slowly varying step curvature we separate these space variables into fast (η) and slow (σ) to reduce the adatom diffusion equation between non-parallel steps to a 1D equation; and we solve this equation for the adatom density and flux. Similar considerations are briefly discussed in [9] without reference to any specific coordinate system. Third, we define the discrete step chemical potential for nearest-neighbor, dipole and entropic step repulsions. Fourth, we describe the velocity of each step edge.

The geometry consists of descending, non-intersecting steps with height a, which are numbered $i = 1, 2, \ldots, N$ and surround a top terrace; cf. Fig. 3.1. The projection of step edges on the high-symmetry ("basal") plane of the crystal is a family of smooth curves ([3]) described by the position vector $\mathbf{r}(\eta, \sigma; t)$: The variable η corresponds to the radius $r = r_i$ of Sec. 2.2.1 with $\eta = \eta_i$ (and $\mathbf{r} = \mathbf{r}_i$) for the ith edge and $\eta_i < \eta < \eta_{i+1}$ for the ith terrace; σ corresponds to the angle in polar coordinates and increases counterclockwise for definiteness. The unit vectors normal and parallel to step edges in the direction of increasing η and σ are $\mathbf{e}_\eta$ and $\mathbf{e}_\sigma$, taken to be mutually orthogonal, $\mathbf{e}_\eta \cdot \mathbf{e}_\sigma = 0$. The metric coefficients, to be used below, have dimension of length and are typically defined by

$$\xi_\eta = |\partial_\eta \mathbf{r}|, \qquad \xi_\sigma = |\partial_\sigma \mathbf{r}|. \tag{3.1}$$

3.1. Adatom density and vector flux. In this subsection we show that, in correspondence to (2.5) for the case with rotational symmetry, the adatom density, C_i, on the ith terrace satisfies approximately a 1D equation and becomes

$$C_i(\eta,\sigma,t) \sim A_i(\sigma,t)\int_{\eta_i}^{\eta}\frac{\xi_\eta}{\xi_\sigma}\,{\rm d}\eta' + B_i(\sigma,t), \tag{3.2}$$

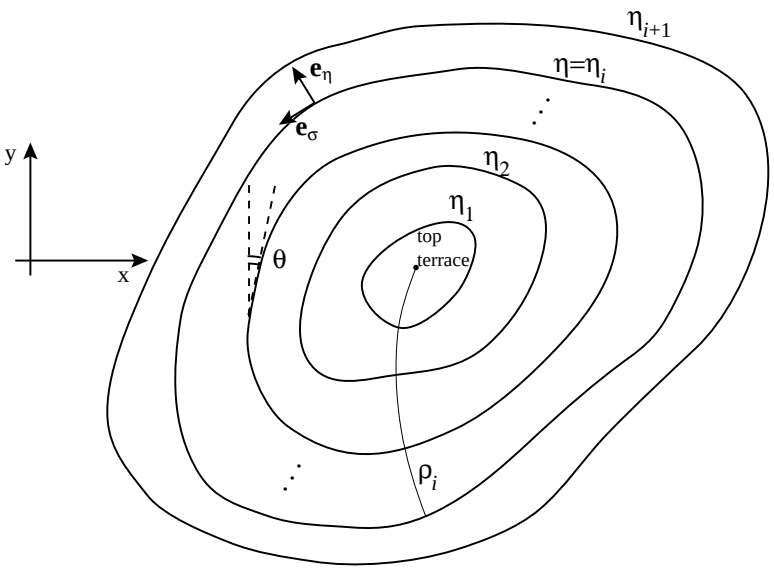

FIG. 3.1. *The geometry of steps near a top terrace in 2+1 dimensions. Contour lines are projections of step edges on the basal plane (x, y) and $\eta = \eta_i$ at the ith edge. The step orientation relative to the crystallographic y axis is indicated by the angle θ. The length ρ_i is defined by (3.17).*

where A_i and B_i are determined from boundary conditions for atom attachment-detachment at steps as discussed below. We also describe the vector-valued adatom flux on the ith terrace, $\mathbf{J}_i = -D_s \nabla C_i$.

We proceed to derive (3.2). The diffusion equation (2.1) with $F = 0$ and the quasi-steady approximation reduces to the Laplace equation, $\Delta C_i = 0$, where Δ denotes the Laplacian. In the local coordinate system, where $\nabla = (\xi_\eta^{-1}\partial_\eta, \xi_\sigma^{-1}\partial_\sigma) \equiv (\partial_\perp, \partial_\parallel)$,

$$(\xi_\eta\, \xi_\sigma)^{-1}\left[\partial_\eta\left(\frac{\xi_\sigma}{\xi_\eta}\,\partial_\eta C_i\right) + \partial_\sigma\left(\frac{\xi_\eta}{\xi_\sigma}\,\partial_\sigma C_i\right)\right] = 0 \qquad \eta_i < \eta < \eta_{i+1}. \tag{3.3}$$

We solve (3.3) for slowly varying step curvature by considering variations of C_i with σ small compared to its variations with η. Thus, by neglecting derivatives with respect to σ we reduce (3.3) to the 1D equation

$$(\xi_\eta\, \xi_\sigma)^{-1}\,\partial_\eta\left(\frac{\xi_\sigma}{\xi_\eta}\,\partial_\eta C_i\right) = 0, \tag{3.4}$$

which becomes (2.5) in rotational symmetry, where $\xi_\eta = $ const. and $\xi_\sigma = r$. Equation (3.2) follows by direct integration of (3.4). Note that $C_i = B_i$ at $\eta = \eta_i$.

Next, we obtain $\mathbf{J}_i = \mathbf{e}_\eta\, J_{i,\perp} + \mathbf{e}_\sigma\, J_{i,\parallel}$ and C_i via determining A_i and B_i from the conditions of atom attachment-detachment at $\eta = \eta_i$ and η_{i+1}, the step edges bounding the ith terrace. By analogy with (2.6), these conditions are

$$-J_{i,\perp} = k_u\left(C_i - C_i^{eq}\right) \quad \eta = \eta_i, \quad J_{i,\perp} = k_d\left(C_i - C_{i+1}^{eq}\right) \quad \eta = \eta_{i+1}, \tag{3.5}$$

where $J_{i,\perp} = -D_s \partial_\perp C_i$ denotes the transverse (η-) component of the adatom flux. By (3.2) and (3.5), the restrictions on the ith step edge of $J_{i,\perp}$ and $J_{i,\parallel} = -D_s \partial_\parallel C_i$, the longitudinal ($\sigma$-) component of the adatom flux, are found to be

$$J_{i,\perp}|_i = -\frac{D_s}{\xi_\sigma|_i}\, A_i, \tag{3.6}$$

$$J_{i,\parallel}|_i = -\frac{D_{\rm s}}{\xi_\sigma|_i}\,\partial_\sigma B_i, \tag{3.7}$$

where $Q|_i$ denotes the value, $Q(\eta=\eta_i)$, of Q at $\eta=\eta_i$ throughout this article,

$$A_i = \frac{C_{\rm s}}{k_{\rm B}T}\,\frac{\mu_{i+1}-\mu_i}{D_{\rm s}\left(\dfrac{1}{k_{\rm u}}\dfrac{1}{\xi_\sigma|_i}+\dfrac{1}{k_{\rm d}}\dfrac{1}{\xi_\sigma|_{i+1}}\right)+\displaystyle\int_{\eta_i}^{\eta_{i+1}}\frac{\xi_\eta}{\xi_\sigma}\,{\rm d}\eta}, \tag{3.8a}$$

$$B_i = \frac{D_{\rm s}\left(\dfrac{1}{k_{\rm u}}\,\dfrac{C_{i+1}^{\rm eq}}{\xi_\sigma|_i}+\dfrac{1}{k_{\rm d}}\,\dfrac{C_i^{\rm eq}}{\xi_\sigma|_{i+1}}\right)+C_i^{\rm eq}\displaystyle\int_{\eta_i}^{\eta_{i+1}}\frac{\xi_\eta}{\xi_\sigma}\,{\rm d}\eta}{D_{\rm s}\left(\dfrac{1}{k_{\rm d}}\dfrac{1}{\xi_\sigma|_{i+1}}+\dfrac{1}{k_{\rm u}}\dfrac{1}{\xi_\sigma|_i}\right)+\displaystyle\int_{\eta_i}^{\eta_{i+1}}\frac{\xi_\eta}{\xi_\sigma}\,{\rm d}\eta}, \tag{3.8b}$$

and we used (2.3) by setting $\mu^{\rm st}=\mu_i$, the chemical potential at the ith step edge. The density C_i is then determined in terms of $C_i^{\rm eq}$ and $C_{i+1}^{\rm eq}$ via (3.2) and (3.8).

The continuum limits of (3.6)–(3.8) are carried out in Sec. 4.1. Evidently, in rotational symmetry ($\xi_\eta=$ const., $\xi_\sigma|_i=r_i$) formula (3.6) with (3.8a) reduces exactly to the radial current $J_i(r=r_i,t)$ of (2.7).

3.2. Discrete step chemical potential. In this subsection we define and then determine the step chemical potential, μ_i, of the ith step edge. First, we relate μ_i with the step curvature when the step energy per length is independent of the step orientation. Second, we provide an explicit formula for μ_i in the case with nearest-neighbor, dipole and entropic step repulsions.

3.2.1. Relation with step edge curvature. We next show that $\mu_i(\sigma,t)$ is related to the curvature, κ_i, of the ith step edge by the formula

$$\mu_i = \frac{\Omega}{a}\left(\frac{1}{\xi_\eta|_i}\,\partial_{\eta_i}U_i+\kappa_i\,U_i\right),\qquad \xi_\eta|_i\equiv\xi_\eta|_{\eta=\eta_i}, \tag{3.9}$$

where U_i is the total energy per length of the ith step edge, which is a function of η_i independent of the step orientation; cf. Sec. 5.2 for extensions to more general U_i.

First, we provide a formal definition of μ_i, the change of the step energy by addition or removal of an atom to or from the step edge at $\eta=\eta_i$. We consider a properly short length ${\rm d}s=\xi_\sigma|_i{\rm d}\sigma$ of the ith edge, which has energy $U_i\,{\rm d}s$. Attachment and detachment of atoms results in the shift of η_i by ${\rm d}\eta$, the motion of the step edge along its local normal by ${\rm d}\rho\equiv\xi_\eta|_i{\rm d}\eta$, and the change of the step energy $U_i{\rm d}s$ by ${\rm d}_\eta(U_i{\rm d}\sigma)$, where the shift operator ${\rm d}_\eta$ is defined by ${\rm d}_\eta Q\equiv Q|_{\eta+{\rm d}\eta}-Q|_\eta$. Hence,

$$\mu_i \equiv \frac{\Omega}{a}\,\frac{{\rm d}_\eta(U_i{\rm d}s)}{{\rm d}\rho\,{\rm d}s} = \frac{\Omega}{a}\left[\xi_\eta^{-1}\partial_{\eta_i}U_i+U_i\,(\xi_\sigma\xi_\eta)^{-1}\partial_\eta\xi_\sigma\right]\qquad \eta=\eta_i. \tag{3.10}$$

Second, we simplify (3.10) via elementary differential geometry, by which ([11]) $\partial_\perp\xi_\sigma=\kappa\xi_\sigma$ where κ is the curvature of the curve $\mathbf{r}(\eta,\sigma,t)$ with $\eta=$ const. and $\partial_\perp=\xi_\eta^{-1}\partial_\eta$. Thus,

$$\partial_\eta\xi_\sigma = \kappa\,\xi_\sigma\,\xi_\eta. \tag{3.11}$$

The combination of (3.10) and (3.11) yields (3.9).

We note in passing that, by using $\kappa = \nabla \cdot \mathbf{e}_\eta$ and viewing U_i as the restriction to $\eta = \eta_i$ of a differentiable function U of η, (3.9) is recast to

$$\mu_i(\sigma, t) = \frac{\Omega}{a}\, \nabla \cdot (U\, \mathbf{e}_\eta) \qquad \text{at } \eta = \eta_i. \tag{3.12}$$

This equation asserts that μ_i is the value at $\eta = \eta_i$ of the continuous function $\tilde{\mu}(\eta, \sigma, t) = (\Omega/a)\nabla \cdot (U\mathbf{e}_\eta)$, which is defined by the right side of (3.12).

3.2.2. Nearest-neighbor, dipole and entropic step interactions. We next relate μ_i with the step edge positions η_j by specifying the step edge energy per unit length, U_i. We consider two contributions to U_i: (i) the step line tension γ, i.e., the energy per unit length of an isolated step by neglecting step orientation dependence; and (ii) the interaction energy with other steps, $U_i^{\rm int}$. Thus,

$$U_i = \gamma + U_i^{\rm int}, \tag{3.13}$$

where γ is a constant, and $U_i^{\rm int}$ depends on η_i and the positions η_j $(j \neq i)$ of steps interacting with the ith edge; cf. Sec. 5.2 for inclusion of step orientation dependence.

In particular, we show by using (3.9) and (3.13) via suitable definitions and notation that for nearest-neighbor, dipole and entropic step repulsions μ_i is given by

$$\begin{aligned} \mu_i = \frac{\Omega}{a}\,\gamma\kappa_i + \frac{\Omega}{a}\,\frac{1}{3}\,g \Bigg\{ & \frac{2}{a}\,[m_i^3\,\Phi(\zeta_i, \zeta_{i+1}) - m_{i-1}^3\,\Phi(\zeta_i, \zeta_{i-1})] \\ & + \frac{1}{\lambda}\,[m_i^2\,\partial_{\zeta_i}\Phi(\zeta_i, \zeta_{i+1}) + m_{i-1}^2\,\partial_{\zeta_i}\Phi(\zeta_i, \zeta_{i-1})] \\ & + \kappa_i\,[m_i^2\,\Phi(\zeta_i, \zeta_{i+1}) + m_{i-1}^2\,\Phi(\zeta_i, \zeta_{i-1})] \Bigg\}. \end{aligned} \tag{3.14}$$

The notation in (3.14) is briefly explained as follows. By analogy with (2.8) and (2.9) of Sec. 2.2.1, g is the step-step interaction strength, $g > 0$, ζ_j are local, non-dimensional coordinates analogous to the radii r_j of circular steps, m_i is the (discrete) step density at the ith step, λ is a macroscopic length, and $\Phi(\zeta, \chi)$ is a geometrical factor that reduces to $\frac{2\chi}{\zeta+\chi}$ for circular steps; cf. (2.9). We now define more precisely the parameters g and λ and the variables m_j, ζ_j and Φ in order to derive (3.14).

First, by direct comparison with (2.9), the interaction energy, $U_i^{\rm int}$, is replaced by

$$U^{\rm int} = g\,(V_{i,i+1} + V_{i,i-1}), \tag{3.15}$$

where g is the positive interaction strength (energy/length), and $V_{i,i\pm1}$ corresponds to the interaction between the ith and $(i \pm 1)$th steps and depends on η_i and $\eta_{i\pm1}$. To stress the length scales involved, we specify that $V_{i,i\pm1}$ depend on the macroscopic lengths ρ_i and $\rho_{i\pm1}$, and the microscopic width of the ith or $(i-1)$th terrace, $|\rho_i - \rho_{i\pm1}|$,

$$V_{i,i+1} = \tilde{V}(\delta\rho_i, \rho_i, \rho_{i+1}), \qquad V_{i,i-1} = \tilde{V}(\delta\rho_{i-1}, \rho_i, \rho_{i-1}), \tag{3.16}$$

where $\tilde{V}$ is thought of as the leading-order term of a small-curvature expansion for realistic, step shape dependent interactions; here, $\delta\rho_i = \rho_{i+1} - \rho_i$, $\delta\rho_{i-1} = \rho_i - \rho_{i-1}$,

$$\rho_i = \rho|_{\eta=\eta_i}, \qquad \rho = \int_{\eta_0}^{\eta} \xi_{\eta'}\, {\rm d}\eta', \tag{3.17}$$

and $\eta_0 = 0$ for definiteness (cf. Fig. 3.1); in axisymmetry, $\rho = r$. We assume that the variations of $V_{i,i+1}$ with $\delta\rho_i$ are large compared to its variations with ρ_i and ρ_{i+1}, and also suppress the trivial dependence of $\tilde{V}$ on the coordinate σ.

Second, we simplify $V_{i,i\pm1}$ for dipole and entropic step interactions ([23]). By analogy with (2.9) for circular steps and use of non-dimensional variables, we define

$$V_{i,i+1} = \frac{1}{3}\, m_i^2\, \Phi(\zeta_i, \zeta_{i+1}), \qquad V_{i,i-1} = \frac{1}{3}\, m_{i-1}^2\, \Phi(\zeta_i, \zeta_{i-1}), \tag{3.18}$$

where

$$m_i = \frac{a}{\delta\rho_i}, \qquad \delta\rho_i = \rho_{i+1} - \rho_i, \tag{3.19}$$

is the (discrete) step density at the ith step, the non-dimensional ζ_i is defined by

$$\zeta_i = \zeta|_{\eta=\eta_i}, \quad \zeta = \frac{\rho}{\lambda}, \tag{3.20}$$

λ denotes the macroscopic length over which the step density m_i varies ($\lambda \gg a$), and $\Phi(\zeta, \chi)$ is a geometrical factor with $\partial_\zeta \Phi = O(1)$ and $\partial_\chi \Phi = O(1)$ at $\zeta = \zeta_i = \rho_i/\lambda$ and $\chi = \zeta_{i+1} = \rho_{i+1}/\lambda$; cf. Sec. 5.1 for more general interactions. For bi-periodic profiles λ is taken to be the smaller of the two wavelengths. The terrace width $\delta\rho_i$ is considered $O(a)$ or larger, and the step radius of curvature κ_i^{-1} and length ρ_i are $O(\lambda)$ or larger. The factor $1/3$ is included in (3.18) for later algebraic convenience.

The step chemical potential μ_i is then determined by combination of (3.9) with definitions (3.13), (3.15) and (3.18). After some algebra we obtain (3.14). The reader can verify directly that with rotational symmetry and $\Phi(\zeta, \chi) = 2\chi/(\zeta + \chi)$, (3.14) reduces exactly to (2.8) and (2.9).

A word of caution about the nature of the step-step interaction term $V_{i,i+1}$ is in order. Because $V_{i,i+1}$ represents the interaction energy per unit length of the ith step with the entire $(i+1)$th step, physically admissible interactions should satisfy

$$V_{i,i+1}\, \mathrm{d}s_i = V_{i+1,i}\, \mathrm{d}s_{i+1}, \tag{3.21}$$

where $\mathrm{d}s_i = \xi_\sigma|_i\, \mathrm{d}\sigma$ is a properly short length of the ith step edge. Condition (3.21) stems from viewing the interaction energy $V_{i,i+1}\mathrm{d}s_i$ entering (3.15) as a "two-body potential", which is invariant under the interchange of two edges. Hence, the Φ of (3.18) cannot be arbitrary. For example, $\Phi \equiv$const. violates (3.21) for non-straight steps since ξ_σ varies with η. In Appendix A we derive consistency conditions for $V_{i,i+1}$ on the basis of (3.21). These conditions are invoked in the continuum limit of Sec. 4.2.

3.3. Step velocity law. In this subsection we conclude our formulation of the discrete step-flow equations in 2+1 dimensions by describing in the local coordinates (η, σ) the step velocity law, which expresses mass conservation for atoms by analogy with (2.10) of the radial case. If the major transport processes are diffusion of adatoms across terraces and attachment-detachment of atoms at steps by neglect of atom diffusion along step edges, the (normal) velocity of the ith step is

$$v_i \equiv \mathbf{e}_\eta \cdot \frac{d\mathbf{r}_i}{dt} = \frac{\Omega}{a}\left[\mathbf{J}_{i-1}(\eta, \sigma, t) - \mathbf{J}_i(\eta, \sigma, t)\right] \cdot \mathbf{e}_\eta = \frac{\Omega}{a}(J_{i-1,\perp} - J_{i,\perp}) \quad \eta = \eta_i. \tag{3.22}$$

4. Continuum limit in 2+1 dimensions. In this section we derive macroscopic evolution laws from the microscopic step flow equations of Sec. 3, where no material deposition is included ($F = 0$). After introducing basic conditions for the continuum limit, we consider the BCF-type ingredients in due order, by analogy with the procedure of Sec. 2.2.2 for circular steps, and combine them to obtain a PDE for the surface height profile. We also discuss alternative derivations of the continuum equations via a weak formulation and a surface free-energy consideration.

We start with a few general comments on the continuum approach. The coarse graining applied here is meaningful if the terrace width, $\delta\rho_i \geq O(a)$, is much smaller than: (i) the length, λ, over which the step density varies; (ii) the step radius of curvature, κ_i^{-1}; and (iii) the length over which the step edge curvature varies, estimated by the mean value of $|\kappa_i/\partial_s\kappa_i|$. The continuum limit is formally attained by

$$\frac{a}{\lambda} \to 0. \tag{4.1}$$

The lengths ξ_σ and ξ_η are $O(\lambda)$ and, thus, the continuum limit is approached via

$$\delta\eta_i = \eta_{i+1} - \eta_i \sim \delta\rho_i\, \xi_\eta^{-1} = O\left(\frac{a}{\lambda}\right) \to 0 \tag{4.2}$$

by keeping the step density m_i and the kinetic parameter q of (2.12) fixed,

$$m_i = \frac{a}{\delta\rho_i} = O(1), \qquad q = \frac{D_\mathrm{s}}{ka} = O(1), \tag{4.3}$$

which implies that $q < O(\lambda/a)$, or $D_\mathrm{s}/k < O(\lambda)$; the same conditions are assumed to apply if the kinetic rate k is replaced by k_u or k_d.

By (4.1) and (4.2) the following statements hold by analogy with Sec. 2.2.2 in rotational symmetry ([30]). (i) The step density approaches the surface slope,

$$m_i \to m = |\nabla h| = O(1). \tag{4.4}$$

(ii) The unit vector, $\mathbf{e}_\eta|_i$, normal to ith step edge becomes

$$\mathbf{e}_\eta|_i \to \mathbf{e}_\eta = -\frac{\nabla h}{|\nabla h|}. \tag{4.5}$$

(iii) The step curvature, $\kappa_i = \nabla \cdot \mathbf{e}_\eta|_i$, approaches

$$\kappa_i \to \kappa = -\nabla \cdot \left(\frac{\nabla h}{|\nabla h|}\right). \tag{4.6}$$

(iv) The step normal velocity, $v_i = \mathbf{e}_\eta \cdot d\mathbf{r}_i/dt$, becomes

$$v_i \to v(\mathbf{r}, t) = \frac{\partial_t h}{|\nabla h|}. \tag{4.7}$$

The last relation is obtained by differentiation of $h(\mathbf{r}_i(t), t) = \text{const.}$ with respect to time, t, where $\mathbf{r}_i(t)$ is the position vector for the ith step edge, and use of (4.5). In the right sides of (4.4)–(4.7) we have set $\eta = \eta_i$.

To clarify the notation of this section, $Q|_i$ denotes the value $Q(\eta = \eta_i)$ suppressing σ, while $Q|_{i,\breve{\sigma}}$ specifies $Q = Q(\eta_i, \sigma = \breve{\sigma})$. This notation is used for $Q = J_{i,\perp}$ and $Q = J_{i,\parallel}$, the adatom flux transverse and longitudinal components.

4.1. Surface current. In this subsection we show that the continuum surface current, $\mathbf{J}(\mathbf{r},t)$, is related to the continuum step chemical potential, $\mu(\mathbf{r},t)$, by

$$\mathbf{J}(\mathbf{r},t) = -C_{\rm s}\,\mathbf{M}\cdot\nabla\mu, \tag{4.8}$$

where $\mathbf{M}$ is the surface mobility, in principle a second-rank tensor. In the local coordinates (η,σ), where $\mathbf{J}$ and $\nabla\mu = (\nabla_\perp + \nabla_\parallel)\mu$ are the column vectors

$$\mathbf{J} = \begin{pmatrix} J_\perp \\ J_\parallel \end{pmatrix}, \quad \nabla\mu = \begin{pmatrix} \partial_\perp\mu \\ \partial_\parallel\mu \end{pmatrix}, \quad \partial_\perp \equiv \mathbf{e}_\eta\cdot\nabla = \xi_\eta^{-1}\partial_\eta,\ \partial_\parallel \equiv \mathbf{e}_\sigma\cdot\nabla = \xi_\sigma^{-1}\partial_\sigma, \tag{4.9}$$

$\mathbf{M}$ is found to be represented by the 2×2 matrix

$$\mathbf{M} = \frac{D_{\rm s}}{k_{\rm B}T}\,\mathbf{\Lambda}, \quad \mathbf{\Lambda} = \begin{pmatrix} \dfrac{1}{1+q\,|\nabla h|} & 0 \\ 0 & 1 \end{pmatrix}, \tag{4.10}$$

and q is defined as in the rotationally symmetric case; cf. (2.12).

We proceed to derive (4.8) and (4.10) with attention to the assumptions involved in the coarse graining for the adatom flux. While the continuum step chemical potential, $\mu(\mathbf{r},t)$, is simply the continuous extension of the right side of (3.12), $\mu(\mathbf{r},t) = \tilde{\mu}(\eta_i,\sigma,t)$ as $\eta_{i+1}\to\eta_i$, the continuum surface current $\mathbf{J}(\mathbf{r},t)$ is here defined to stem from $\mathbf{J}_i(\eta=\eta_i,\sigma,t)$. The continuum limit obtained for $\mathbf{J}$ is independent of the choice of the point of evaluation for $\mathbf{J}_i$ if

$$|\mathbf{J}_i(\eta_{i+1}) - \mathbf{J}_i(\eta_i)| = O\!\left(\frac{a}{\lambda}\,|\mathbf{J}_i(\eta_i)|\right) \qquad \frac{a}{\lambda}\to 0, \tag{4.11}$$

where the dependence on (σ,t) is suppressed. The definition of the coarse-grained current, $\mathbf{J}$, and condition (4.11) are modified in the presence of deposition ([31]).

Next, we invoke the separation of the local space variables (η,σ) into fast and slow, which was introduced in Sec. 3.1, in order to derive formulas for the continuum adatom flux. This approximation is valid for sufficiently small step edge curvature variation. An alternative derivation in terms of Taylor expansions is provided elsewhere ([29]). First, we determine $J_\perp(\mathbf{r},t)$, the adatom flux normal to step edges, as the appropriate limit of $J_{i,\perp}|_i$, the restriction on the ith step edge of the transverse adatom current on the ith terrace. By (3.6) and (3.8a), we apply the approximations

$$\int_{\eta_i}^{\eta_{i+1}} \frac{\xi_\eta}{\xi_\sigma}\,{\rm d}\eta = \frac{\xi_\eta|_i}{\xi_\sigma|_i}\,\delta\eta_i + O[(\delta\eta_i)^2], \tag{4.12}$$

$$\frac{1}{k_{\rm u}}\frac{1}{\xi_\sigma|_i} + \frac{1}{k_{\rm d}}\frac{1}{\xi_\sigma|_{i+1}} = \left(\frac{1}{k_{\rm u}} + \frac{1}{k_{\rm d}}\right)\frac{1}{\xi_\sigma|_i}\,[1+O(\delta\eta_i)], \quad \delta\eta_i = \eta_{i+1}-\eta_i \to 0. \tag{4.13}$$

Thus, the coefficient A_i of (3.8a) becomes

$$A_i = \frac{C_{\rm s}}{k_{\rm B}T}\,\frac{\mu_{i+1}-\mu_i}{q\,(\xi_\sigma|_i)^{-1} + (\xi_\eta/\xi_\sigma)|_i\,\delta\eta_i}[1+O(\delta\eta_i)], \tag{4.14}$$

where $\mu_i = \tilde{\mu}(\eta=\eta_i,\sigma,t)$ and

$$\mu_{i+1}-\mu_i = \delta\eta_i\,\frac{\partial\tilde{\mu}}{\partial\eta}\,[1+O(\delta\eta_i)] \qquad \eta=\eta_i. \tag{4.15}$$

Hence, (3.6) for $J_{i,\perp}$ at $\eta = \eta_i$ readily becomes

$$J_{i,\perp}|_i = -\frac{D_{\rm s}\, C_{\rm s}}{k_{\rm B}T}\,\frac{1}{\xi_\eta|_i}\,\frac{\dfrac{\tilde\mu(\eta_{i+1},\sigma,t)-\tilde\mu(\eta_i,\sigma,t)}{\delta\eta_i}}{1+q\,\dfrac{a}{\delta\eta_i\,\xi_\eta|_i}}\left[1+O\!\left(\frac{a}{\lambda}\right)\right]$$

$$\to \mathbf{J}(\mathbf{r},t)\cdot\mathbf{e}_\eta = J_\perp(\mathbf{r},t) = -\frac{D_{\rm s}\, C_{\rm s}}{k_{\rm B}T}\,\frac{1}{1+q\,|\nabla h|}\;\partial_\perp\mu \qquad \delta\eta_i\to 0. \tag{4.16}$$

Second, we obtain a formula for $J_\parallel(\mathbf{r},t)$, the continuum-scale adatom flux parallel to step edges on the basal plane, as a limit of $J_{i,\parallel}|_i$, the restriction on the ith step edge of the longitudinal adatom current on the ith terrace. By (3.7) and (3.8b), we apply the approximation

$$\frac{1}{k_{\rm u}}\,\frac{C_{i+1}^{\rm eq}}{\xi_\sigma|_i}+\frac{1}{k_{\rm d}}\,\frac{C_i^{\rm eq}}{\xi_\sigma|_{i+1}} = \frac{C_i^{\rm eq}}{\xi_\sigma|_i}\left(\frac{1}{k_{\rm u}}+\frac{1}{k_{\rm d}}\right)[1+O(\delta\eta_i)], \tag{4.17}$$

and reduce the B_i of (3.8b) to

$$B_i = C_i^{\rm eq}[1+O(a/\lambda)]. \tag{4.18}$$

Hence, by (3.2) the adatom density C_i at the ith step edge ($\eta=\eta_i$) is

$$C_i(\eta_i,\sigma,t) = C_i^{\rm eq}[1+O(a/\lambda)]. \tag{4.19}$$

The coarse graining is effected only through η because the atomic length a is introduced in the η-direction via $\xi_\eta|_i\,\delta\eta_i = O(a)$ allowing σ to vary continuously. Thus, (4.18) and (4.19) can be differentiated with respect to σ to obtain $J_{i,\parallel}$ at $\eta=\eta_i$. Hence, (3.7) reads

$$J_{i,\parallel}|_i = -D_{\rm s}\,\frac{1}{\xi_\sigma|_i}\,\partial_\sigma C_i(\eta_i,\sigma,t) = -\frac{D_{\rm s}C_{\rm s}}{k_{\rm B}T}\,\frac{1}{\xi_\sigma|_i}\,\partial_\sigma\tilde\mu(\eta_i,\sigma,t)\left[1+O\!\left(\frac{a}{\lambda}\right)\right]$$

$$\to \mathbf{J}(\mathbf{r},t)\cdot\mathbf{e}_\sigma = J_\parallel(\mathbf{r},t) = -\frac{D_{\rm s}C_{\rm s}}{k_{\rm B}T}\;\partial_\parallel\mu \qquad \delta\eta_i\to 0, \tag{4.20}$$

where we used (2.3) to relate $C_i^{\rm eq}$ with $\mu^{\rm st} = \mu_i = \tilde\mu(\eta_i,\sigma,t)$. Equations (4.8)–(4.10) then follow from (4.16) and (4.20) with $\mathbf{J} = \mathbf{e}_\eta\,J_\perp + \mathbf{e}_\sigma\,J_\parallel$ where, in the local coordinates (η,σ), $\mathbf{e}_\eta = (1\quad 0)^{\rm T}$ and $\mathbf{e}_\sigma = (0\quad 1)^{\rm T}$; $\mathbf{V}^{\rm T}$ denotes the transpose of $\mathbf{V}$. Note that the mobility tensor of (4.10) has a structure similar to that of the tensor given by Eq. (63) in [9], where the anisotropy is due to the imposed atom diffusion along step edges. We emphasize that condition (4.11) is satisfied throughout and, thus, $\mathbf{J}$ is herein obtained unambiguously for surface relaxation.

Formulas (4.8) and (4.10), once derived, admit a relatively simple interpretation. The transverse adatom flux, $J_\perp$, which participates in the boundary conditions for atom attachment-detachment at steps, is restricted by the terrace width and, thus, has a slope-dependent scalar mobility. By contrast, the longitudinal flux, $J_\parallel$, is set by adatoms that hop freely on each terrace and, thus, has a constant mobility.

Representations of the mobility tensor $\mathbf{M}$ in other coordinate systems can be derived from (4.10). In the basal plane's Cartesian system (x,y), $\mathbf{M}$ is represented by

$$\mathbf{M} = \frac{D_{\rm s}}{k_{\rm B}T}\begin{pmatrix} \dfrac{1}{1+q\,|\nabla h|}\dfrac{(\partial_x h)^2}{|\nabla h|^2}+\dfrac{(\partial_y h)^2}{|\nabla h|^2} & -\dfrac{q|\nabla h|}{1+q|\nabla h|}\dfrac{(\partial_x h)\,(\partial_y h)}{|\nabla h|^2} \\ -\dfrac{q|\nabla h|}{1+q|\nabla h|}\dfrac{(\partial_x h)\,(\partial_y h)}{|\nabla h|^2} & \dfrac{1}{1+q|\nabla h|}\dfrac{(\partial_y h)^2}{|\nabla h|^2}+\dfrac{(\partial_x h)^2}{|\nabla h|^2} \end{pmatrix}, \tag{4.21}$$

which enters (4.8) with $\mathbf{J} = (J_x\ J_y)^{\mathrm{T}}$ and $\nabla = (\partial_x\ \partial_y)^{\mathrm{T}}$ where J_ℓ is the component of $\mathbf{J}$ along the $\ell = x$ or y axis; cf. Appendix B for a derivation of (4.21).

We now comment on the structure of matrix (4.21), particularly the terms $\partial_x h/|\nabla h|$ and $\partial_y h/|\nabla h|$, which are induced by the transformation from local to Cartesian coordinates. Equation (4.21) describes the interplay of: (i) step kinetics, via the term $q\,|\nabla h|$ which measures the ratio of the kinetic length D_{s}/k to the mean terrace width; and (ii) aspect ratio of surface topography, via the ratio $\partial_x h/\partial_y h$ which measures the wavelength ratio for bi-periodic surface profiles. A plausible connection of this interplay to surface relaxation experiments is discussed elsewhere ([29]).

4.2. Continuum step chemical potential. In this subsection we derive the continuum step chemical potential, $\mu(\mathbf{r},t) = \tilde{\mu}(\eta_i,\sigma,t)$, in terms of ∇h, where $h(\mathbf{r},t)$ is the height profile, for the case with dipole and entropic step-step interactions. Specifically, we show by the formulation of Sec. 3.2 that

$$\mu = -\frac{\Omega}{a}\nabla\cdot\left[(\gamma + \tilde{g}\,|\nabla h|^2)\frac{\nabla h}{|\nabla h|}\right], \tag{4.22}$$

where $\tilde{g}$ is a parameter proportional to the interaction strength g; cf. (4.33) with (4.23).

We proceed to derive (4.22) by starting with (3.14), which we simplify in the limit $\delta\eta_i = \eta_{i+1} - \eta_i \to 0$ with fixed step density, m_i. First, we define

$$\Phi_0 \equiv \Phi(\zeta,\zeta), \tag{4.23}$$

a ζ-independent function, and subsequently use the expansion

$$\Phi(\zeta,\chi) \sim \Phi_0 + \partial_\zeta\Phi(\zeta,\chi)|_{\zeta=\chi}\,(\zeta-\chi), \quad \zeta = \zeta_i,\ \chi = \zeta_{i\pm1}, \tag{4.24}$$

recalling that $\zeta = \rho/\lambda$ and ρ is a macroscopic length coordinate; cf. (3.17) and (3.20).

Second, we simplify the bracketed terms of (3.14) via the approximations

$$m_i^3\,\Phi(\zeta_i,\zeta_{i+1}) - m_{i-1}^3\,\Phi(\zeta_i,\zeta_{i-1}) \sim (m_i^3 - m_{i-1}^3)\Phi_0 - 2\,\frac{a}{\lambda}\,m_i^2\,\partial_\zeta\Phi(\zeta,\zeta_i)|_i, \tag{4.25}$$

$$m_i^2\,\partial_{\zeta_i}\Phi(\zeta_i,\zeta_{i+1}) + m_{i-1}^2\,\partial_{\zeta_i}\Phi(\zeta_i,\zeta_{i-1}) \sim 2m_i^2\,\partial_\zeta\Phi(\zeta,\zeta_i)|_i, \tag{4.26}$$

$$m_i^2\,\Phi(\zeta_i,\zeta_{i+1}) + m_{i-1}^2\,\Phi(\zeta_i,\zeta_{i+1}) \sim 2m_i^2\,\Phi_0, \tag{4.27}$$

where $m_i = (a/\lambda)(\delta\zeta_i)^{-1}$, $\delta\zeta_i = \zeta_{i+1} - \zeta_i$, and $Q|_i$ denotes $Q(\zeta_i)$. Thus, (3.14) becomes

$$\begin{aligned}\mu_i \sim \frac{\Omega}{a}\,\gamma\kappa_i + \frac{\Omega}{a}\frac{g}{3}\bigg[&\frac{2}{a}(m_i^3 - m_{i-1}^3)\Phi_0 - \frac{4}{\lambda}m_i^2\partial_\zeta\Phi(\zeta,\zeta_i)|_i \\ &+ \frac{2}{\lambda}m_i^2\partial_\zeta\Phi(\zeta,\zeta_i)|_i + 2\kappa_i m_i^2\Phi_0\bigg],\end{aligned} \tag{4.28}$$

where the ratio of the neglected correction to the right side of (4.28) is $O(a/\lambda)$.

Third, we further simplify μ_i via the approximation

$$m_i^3 - m_{i-1}^3 = (m_i - m_{i-1})(m_i^2 + m_i m_{i-1} + m_{i-1}^2) \sim 3\frac{a}{\lambda}m_i\,\partial_\zeta m|_i, \tag{4.29}$$

where $m_i \to m = |\nabla h||_{\eta=\eta_i}$ by (4.4). Hence, (4.28) becomes

$$\mu_i \sim \frac{\Omega}{a}\,\gamma\kappa_i + \frac{\Omega}{a}\frac{g}{3}\left[\frac{6}{\lambda}\,\Phi_0\,m_i\partial_\zeta m|_i - \frac{2}{\lambda}m_i^2\partial_\zeta\Phi(\zeta,\zeta_i)|_i + 2\kappa_i\Phi_0 m_i^2\right]. \tag{4.30}$$

At this point, we use a consistency relation that stems from condition (3.21) for the step-step interactions. By Proposition A.2 of Appendix A, Φ should satisfy

$$\partial_\zeta \Phi(\zeta,\zeta_i)|_i = -\frac{\lambda\kappa_i}{2}\,\Phi_0. \tag{4.31}$$

Thus, (4.30) is recast to the formula

$$\begin{aligned}\mu_i &\sim \frac{\Omega}{a}\,\gamma\kappa_i + \frac{\Omega}{a}\,g[\partial_\rho(m^2\Phi_0)|_i + \kappa_i m^2\Phi_0]\\ &\to \frac{\Omega}{a}[\gamma\nabla\cdot\mathbf{e}_\eta + g\Phi_0\nabla\cdot(\mathbf{e}_\eta\, m^2)],\end{aligned} \tag{4.32}$$

where we used $\nabla\cdot\mathbf{e}_\eta|_i = \kappa_i$, $\nabla\cdot(f\mathbf{v}) = f\nabla\cdot\mathbf{v} + \mathbf{v}\cdot\nabla f$ for scalar f and vector $\mathbf{v}$, and $\partial_\rho = (\partial_\rho\eta)\,\partial_\eta = \partial_\perp = \mathbf{e}_\eta\cdot\nabla$. Evidently, (4.22) follows from (4.32) via the replacement $\mathbf{e}_\eta = -\nabla h/|\nabla h|$ by (4.5) and the definition

$$\tilde g = g\Phi_0. \tag{4.33}$$

In the axisymmetric case $\Phi_0 = \lim_{r_{i+1}\to r_i} \frac{2r_{i+1}}{r_i+r_{i+1}} = 1$, which yields $\tilde g = g$; hence, (4.22) for $\mu = \mu(r,t)$ reduces to (2.14). In Sec. 4.5.1 we derive (4.22) via an alternative formulation based on a variational principle.

4.3. Mass conservation law. Next, we derive from the step velocity law (3.22) the familiar mass conservation statement for atoms,

$$\partial_t h + \Omega\nabla\cdot\mathbf{J} = 0, \tag{4.34}$$

where $h(\mathbf{r},t)$ is the continuum-scale height profile and $\mathbf{J}$ is the surface (adatom) current. We follow the corresponding derivation of Sec. 2.2.2 for the radial case, invoking the identity $\nabla\cdot\mathbf{J}_i = 0$ for $\eta_i < \eta < \eta_{i+1}$, i.e., the property that the net adatom flux through any closed curve lying entirely on a terrace is zero. By starting with (3.22) and the definition $\mathbf{J}(\mathbf{r},t) = J_i(\eta_i,\sigma,t)$ as $\eta_{i+1}\to\eta_i$, we next relate $J_{i-1,\perp}$ at the ith step edge, $\eta = \eta_i$, with $J_{i-1,\perp}$ and $J_{i-1,\parallel}$ at the $(i-1)$th edge, $\eta = \eta_{i-1}$.

First, we integrate $\nabla\cdot\mathbf{J}_i = 0$ with respect to η on (η_i,η_{i+1}). Thus, we obtain

$$(\xi_\sigma J_{i,\perp})|_{i+1} - (\xi_\sigma J_{i,\perp})|_i + \partial_\sigma \int_{\eta_i}^{\eta_{i+1}} \xi_\eta J_{i,\parallel}\,\mathrm{d}\eta = 0. \tag{4.35}$$

Further integration of (4.35) with respect to σ over the interval $(\breve\sigma,\breve\sigma+\delta\sigma)$ for arbitrary $\breve\sigma$, sufficiently small $\delta\sigma$ and $\delta\eta_i = \eta_{i+1} - \eta_i$ yields

$$J_{i,\perp}|_{i+1,\breve\sigma} = \frac{\xi_\sigma|_{i,\breve\sigma}}{\xi_\sigma|_{i+1,\breve\sigma}}\,J_{i,\perp}|_{i,\breve\sigma} - \frac{\delta\eta_i}{\delta\sigma}\,\frac{1}{\xi_\sigma|_{i,\breve\sigma}}\,[(\xi_\eta\,J_{i,\parallel})|_{i,\breve\sigma+\delta\sigma} - (\xi_\eta\,J_{i,\parallel})|_{i,\breve\sigma}]. \tag{4.36}$$

Second, we simplify the step velocity (3.22) by (4.36) via shifting i to $i-1$,

$$\begin{aligned}v_i &= \frac{\Omega}{a}\left\{\frac{\xi_\sigma|_{i-1,\breve\sigma}}{\xi_\sigma|_{i,\breve\sigma}}\,J_{i-1,\perp}|_{i-1,\breve\sigma} - J_{i,\perp}|_{i,\breve\sigma}\right.\\ &\qquad\left. - \frac{\delta\eta_i}{\delta\sigma}\,\frac{1}{\xi_\sigma|_{i,\breve\sigma}}\,[(\xi_\eta\,J_{i-1,\parallel})|_{i,\breve\sigma+\delta\sigma} - (\xi_\eta J_{i-1,\parallel})|_{i,\breve\sigma}]\right\}\\ &= -\frac{\Omega}{a}\,\frac{\xi_\eta|_{i,\breve\sigma}\,\delta\eta_i}{\xi_\sigma|_{i,\breve\sigma}\,\xi_\eta|_i}\left\{\frac{-\xi_\sigma|_{i-1,\breve\sigma}\,J_{i-1,\perp}|_{i-1,\breve\sigma} + J_{i,\perp}|_{i,\breve\sigma}\,\xi_\sigma|_{i,\breve\sigma}}{\delta\eta_i}\right.\\ &\qquad\left. + \frac{\xi_\eta|_{i,\breve\sigma+\delta\sigma}\,J_{i-1,\parallel}|_{i,\breve\sigma+\delta\sigma} - \xi_\eta|_{i,\breve\sigma}\,J_{i-1,\parallel}|_{i,\breve\sigma}}{\delta\sigma}\right\}.\end{aligned} \tag{4.37}$$

In the limit $(\delta\eta_i, \delta\sigma) \to (0,0)$, v_i approaches the right side of (4.7) and $\xi_\eta|_{i,\check{\sigma}}\delta\eta_i/a \to |\nabla h|^{-1}|_{\eta=\eta_i}$. Thus, (4.37) reduces to

$$\partial_t h = -\Omega \frac{1}{\xi_\sigma\, \xi_\eta}[\partial_\eta(\xi_\sigma J_\perp) + \partial_\sigma(\xi_\eta J_\parallel)], \tag{4.38}$$

which is identified with (4.34) in the local coordinates, where $\nabla = (\xi_\eta^{-1}\partial_\eta, \xi_\sigma^{-1}\partial_\sigma)$. In Sec. 4.5.2 we derive (4.34) by an alternative formulation based on weak solutions.

4.4. Evolution equation for height profile. In this subsection we combine the evolution laws of the previous sections for the surface current, $\mathbf{J}$, step chemical potential, μ, and velocity $\partial_t h$ in order to derive a PDE for the height profile, $h(\mathbf{r}, t)$. A slightly different derivation of this PDE is sketched by one of us in a letter ([29]).

The replacements in (4.34) of $\mathbf{J}$ by (4.8) and μ by (4.22) yield

$$\partial_t h = -B\nabla \cdot \left\{ \mathbf{\Lambda} \cdot \nabla \left[\nabla \cdot \left(\frac{\nabla h}{|\nabla h|} \right) + \frac{g_3}{g_1} \nabla \cdot (|\nabla h| \nabla h) \right] \right\}, \tag{4.39}$$

where $\mathbf{\Lambda}$ is given by (4.10) or (4.21), g_1 and g_3 are

$$g_1 = \frac{\gamma}{a}, \quad g_3 = \frac{\tilde{g}}{a} = \Phi_0 \frac{g}{a}, \tag{4.40}$$

consistent with (2.15) for the radial case where $\Phi_0 = 1$, and the material parameter B is defined by (2.18). For axisymmetric profiles, $h = h(r,t)$, (4.39) readily simplifies to (2.17). We alert the reader that (4.39) has been derived for surface regions around peaks and outside facets. Limitations of this PDE are further discussed in Sec. 6.

4.5. Alternative derivations. In this subsection we provide alternative derivations of continuum evolution laws for surface relaxation by using the formalism of variational formulations and weak solutions. In particular, we show (4.22) for the step chemical potential via a variational formulation and a surface free energy; and (4.34) for mass conservation via a weak formulation. The derivations to be shown here become particularly useful for the extensions of Sec. 5.

A tool that enables alternative derivations is the co-area formula, which converts a two-dimensional integral over the variables (h, s) of surface height, h, and step edge arc length, s, to an integral over the corresponding region of the basal plane (x, y). More precisely, if $\psi(\mathbf{r})$ is a properly integrable function, the co-area formula reads

$$\int \mathrm{d}h \int_{h=\text{const.}} \mathrm{d}s\ \psi(\mathbf{r}) = \int\int \mathrm{d}\mathbf{r}\ \psi(\mathbf{r})\, |\nabla h|, \qquad \mathrm{d}\mathbf{r} \equiv dx\, dy. \tag{4.41}$$

4.5.1. Variational formulation for step chemical potential. We now re-derive (4.22) by following a variational approach. First, we provide an alternative definition of the chemical potential, μ_i, of the ith step edge via an integral formula. Let E^{steps} be the total energy of a step train with a fixed number of steps. By definitions (3.13) and (3.15) for the energy per length of a step,

$$E^{\text{steps}} = \sum_i \int_{L_i} \mathrm{d}s\ (\gamma + g V_{i,i+1}), \tag{4.42}$$

where the summation is over all steps of the given train and L_i is the projection of the ith step edge on the basal plane. Then, μ_i can be defined by the identity

$$\dot{E}^{\text{steps}} = \frac{\mathrm{d}E^{\text{steps}}}{\mathrm{d}t} \equiv \frac{1}{\Omega/a} \sum_i \int_{L_i} \mathrm{d}s\ v_i\, \mu_i(\sigma, t), \tag{4.43}$$

for arbitrary number of steps and contours L_i, where v_i is the step (normal) velocity.

Second, we derive a continuum formula for $\dot{E}^{\rm steps}$ from (4.42). By the replacement

$$\sum_i a \to \int \mathrm{d}h, \tag{4.44}$$

the use of (3.18) for nearest-neighbor interaction terms $V_{i,i+1}$ that pertain to dipole and entropic repulsions, and the application of the co-area formula, (4.41), we obtain

$$E^{\rm steps}[h] = \frac{1}{a}\int\!\!\int_{\mathcal{R}} \mathrm{d}\mathbf{r}\ |\nabla h|\left(\gamma + \frac{g}{3}\Phi_0\,|\nabla h|^2\right), \tag{4.45}$$

where $\Phi_0 = \Phi(\zeta_i,\zeta_i) \sim \Phi(\zeta_i,\zeta_{i+1})$ by (4.23), and $\mathcal{R}$ is the region of the basal plane that consists of the terraces included in $\sum_i$; the boundary, $\partial\mathcal{R}$, of $\mathcal{R}$ corresponds to the first and last edges of the step train. On the basis of (4.45), $E^{\rm steps}$ is viewed as a functional of the height profile, h. The first variation of $E^{\rm steps}$ yields

$$\dot{E}^{\rm steps} = -\frac{1}{a}\int\!\!\int_{\mathcal{R}} \mathrm{d}\mathbf{r}\ \nabla\cdot\left\{\partial_m\left[m\left(\gamma + \frac{g}{3}\Phi_0\,m^2\right)\right]\frac{\nabla h}{|\nabla h|}\right\}\partial_t h, \quad m \equiv |\nabla h|, \tag{4.46}$$

where we applied integration by parts with fixed h on $\partial\mathcal{R}$, i.e., fixed end edges.

Third, we provide an alternative continuum limit for $\dot{E}^{\rm steps}$, this time from the right side of (4.43). Application of the co-area formula to (4.43) results in

$$\dot{E}^{\rm steps} = \Omega^{-1}\int\!\!\int_{\mathcal{R}} \mathrm{d}\mathbf{r}\,|\nabla h|\,v(\mathbf{r},t)\,\mu(\mathbf{r},t), \quad v = \partial_t h/|\nabla h|. \tag{4.47}$$

The comparison of (4.46) and (4.47) for reasonably arbitrary region $\mathcal{R}$ yields

$$\mu(\mathbf{r},t) = -\frac{\Omega}{a}\nabla\cdot\left\{\partial_m\left[m\left(\gamma + \frac{g}{3}\Phi_0\,m^2\right)\right]\frac{\nabla h}{|\nabla h|}\right\}, \quad m = |\nabla h|, \tag{4.48}$$

which is identified with (4.22).

We conclude this section by interpreting (4.48) via a continuum surface free-energy approach. The free energy, G, of a stepped, vicinal surface per unit area of the basal plane is the concave upward, non-analytic function of ∇h defined by ([30])

$$G(|\nabla h|) = g_0 + g_1|\nabla h| + \frac{1}{3}g_3|\nabla h|^3, \tag{4.49}$$

where g_0 accounts for the energy of the basal plane, g_1 is the energy for creating an isolated step (line tension), and g_3 accounts for nearest-neighbor, entropic and dipole repulsions. Thus, (4.45) reads

$$E^{\rm steps} = \int\!\!\int \mathrm{d}\mathbf{r}\ [G(|\nabla h|) - g_0]. \tag{4.50}$$

The first variation of (4.50) yields

$$\dot{E}^{\rm steps} = -\int\!\!\int \mathrm{d}\mathbf{r}\,\nabla\cdot\left[\partial_m G\,\frac{\nabla h}{|\nabla h|}\right]\partial_t h \equiv \Omega^{-1}\int\!\!\int \mathrm{d}\mathbf{r}\,\mu(\mathbf{r},t)\,\partial_t h, \quad m = |\nabla h|, \tag{4.51}$$

by which we obtain (4.48), in agreement with formulas (33) and (34) in [30]. By comparison of (4.45) with (4.50), g_1 and g_3 must be related to γ and g by (4.40).

4.5.2. Weak formulation for mass conservation law. Next, we derive (4.34), the continuum mass conservation law, via a weak formulation based on the co-area formula. For mathematical convenience, the step velocity law (3.22) is stated by

$$v_i = -\frac{\Omega}{a}\,[\mathbf{J}\cdot\mathbf{e}_\eta]_i, \tag{4.52}$$

where $[\mathbf{J}\cdot\mathbf{e}_\eta]_i$ denotes the jump $\{\mathbf{J}_i(\mathbf{r}_i,t)-\mathbf{J}_{i-1}(\mathbf{r}_i,t)\}\cdot\mathbf{e}_\eta$ and $\mathbf{e}_\eta$ is evaluated at $\eta=\eta_i$. We also introduce the quantity

$$I[\varphi] = \sum_i \int_{L_i} \mathrm{d}s\; v_i\,\varphi_i, \tag{4.53}$$

where, similarly to (4.42), the sum is over a step train, and the sequence $\{\varphi_i\}$ approaches an appropriate, reasonably arbitrary test function $\varphi(\mathbf{r})$, $\varphi_i \to \varphi(\mathbf{r})$. We now show that the continuum limit of I has two alternative expressions, which when combined yield (4.34).

First, in view of (4.7), (4.41) and (4.44), the direct limit of I from (4.53) is

$$I[\varphi] = \frac{1}{a}\int\!\!\int_{\mathcal{R}} \mathrm{d}\mathbf{r}\;|\nabla h| v(\mathbf{r},t)\;\varphi(\mathbf{r}) = \frac{1}{a}\int\!\!\int_{\mathcal{R}} \mathrm{d}\mathbf{r}\;(\partial_t h)\;\varphi(\mathbf{r}). \tag{4.54}$$

Second, we derive an alternative limit for I by invoking (4.52) for v_i. Recalling that the surface current $\mathbf{J}(\mathbf{r},t)$ on the basal plane comes from the adatom flux $\mathbf{J}_i$ restricted on the ith step edge where $\nabla\cdot\mathbf{J}_i=0$ on each terrace, we have

$$I[\varphi] = -\frac{\Omega}{a}\int\!\!\int_{\mathcal{R}} \mathrm{d}\mathbf{r}\;(\nabla\cdot\mathbf{J})\,\varphi(\mathbf{r}). \tag{4.55}$$

The comparison of (4.54) and (4.55) yields (4.34) in the weak sense ([14]).

5. Extensions. In this section we provide extensions of the continuum theory developed in Sec. 4 to include more general step interactions due to elastic effects and orientation dependence of step energies. Consequently, we derive modified macroscopic evolution laws the step chemical potential.

5.1. More general, pairwise step interactions. In this subsection we consider pairwise step interactions broader than entropic and dipole interactions yet independent of step orientation. We study: (i) the effects of sufficiently general nearest-neighbor repulsions that satisfy condition (3.21); and (ii) a mathematical model of beyond-nearest-neighbor step interactions. These considerations affect only the discrete step chemical potential, μ_i, leaving intact conditions (3.5) for atom attachment-detachment at steps and the step velocity law (3.22). Thus, we focus on obtaining a modified formula for the continuum step chemical potential, $\mu(\mathbf{r},t)$, to replace (4.22).

5.1.1. General nearest-neighbor repulsions. Next, we show that replacing the step interaction $V_{i,i+1}$ of (3.15) by the general term (3.16) in the form

$$V_{i,i+1} = V(m_i,\zeta_i,\zeta_{i+1}) \tag{5.1}$$

results in the more general continuum formula

$$\mu(\mathbf{r},t) = -\frac{\Omega}{a}\nabla\cdot\left\{[\gamma+g\partial_m(mV_0)]\frac{\nabla h}{|\nabla h|}\right\}, \tag{5.2}$$

where $-\nabla\cdot(\nabla h/|\nabla h|) = \kappa$, the step edge curvature, and $V_0(m) \equiv V(m,\zeta,\zeta)$; cf. (A.3).

We derive (5.2) by two alternative routes. One route relies on the direct coarse graining of Sec. 4.2. By combining (3.9), (3.13), (3.15) and (5.1), we first obtain the discrete step chemical potential of the ith step edge,

$$\begin{aligned}\mu_i = \frac{\Omega}{a}\,\gamma\,\kappa_i + \frac{\Omega}{a}\,g\Big\{&\frac{1}{a}[m_i^2\partial_m V(m_i,\zeta_i,\zeta_{i+1}) - m_{i-1}^2\partial_m V(m_{i-1},\zeta_i,\zeta_{i-1})]\\ &+\frac{1}{\lambda}[\partial_{\zeta_i} V(m_i,\zeta_i,\zeta_{i+1}) + \partial_{\zeta_i} V(m_{i-1},\zeta_i,\zeta_{i-1})]\\ &+\kappa_i[V(m_i,\zeta_i,\zeta_{i+1}) + V(m_{i-1},\zeta_i,\zeta_{i-1})]\Big\},\end{aligned} \tag{5.3}$$

which is an extension of (3.14). The application of approximations entirely similar to (4.25)–(4.30) and use of (A.6) from Appendix A then yields (5.2), which is an extension of (4.22).

Alternatively, we can apply the variational formulation of Sec. 4.5.1. By (4.41), (4.42), (4.44) and (5.1), the continuum-scale energy of steps, $E^{\rm steps}$, is

$$E^{\rm steps}[h] = \frac{1}{a}\int\!\!\int_{\mathcal{R}} {\rm d}\mathbf{r}\ |\nabla h|[\gamma + gV_0(m)], \tag{5.4}$$

with first variation

$$\dot{E}^{\rm steps} = -\frac{1}{a}\int\!\!\int_{\mathcal{R}} {\rm d}\mathbf{r}\ \nabla\cdot\left\{\partial_m[m(\gamma+gV_0)]\,\frac{\nabla h}{|\nabla h|}\right\}\partial_t h, \quad m \equiv |\nabla h|. \tag{5.5}$$

The comparison of (4.47) and (5.5) yields (5.2).

5.1.2. Step interactions beyond nearest neighbors. Next, we consider the effect on the macroscopic evolution laws of pairwise, repulsive step interactions that extend beyond nearest neighbors in the absence of bulk stress ([28, 25, 42]). This consideration again affects only the continuum step chemical potential of Sec. 4.2.

In particular, we show that for a class of elastic step-step interactions including dipole interactions the equations of motion retain their local form in the continuum limit, in agreement with the (1+1)-dimensional case ([42, 48]). This result justifies the formulation of our previous sections where we treat only nearest-neighbor forces between steps. To simplify the analysis but leave intact the essential physics of the problem, we invoke the variational formulation of Sec. 4.5.1.

The starting point is the extension to all other steps of the interaction energy per unit length of the ith step for elastic dipoles in the isotropic form

$$U_i^{\rm int} = \frac{\breve{g}}{2}\sum_{k\neq i}\tilde{\Phi}(\eta_i,\eta_k)\,m_{i,k}^2, \tag{5.6}$$

where the dependence on step orientation is neglected, $\breve{g}$ is the interaction strength for each step pair, $\breve{g} > 0$, the factor $1/2$ is included so that each step pair contributes only once to the sum for $U_i^{\rm int}$, $m_{i,k}$ is defined by

$$m_{i,k} = \frac{\epsilon}{|\zeta_i - \zeta_k|}, \qquad \epsilon = \frac{a}{\lambda}, \tag{5.7}$$

$\zeta_i = \rho_i/\lambda$, and ρ_i is defined by (3.17). We show below that in the continuum limit, $\epsilon \to 0$, the interaction step energy in a region $\mathcal{R}$ of the basal plane becomes

$$E^{\rm int} = \frac{1}{3}g_3\int_{\mathcal{R}} {\rm d}\mathbf{r}\ |\nabla h|^3, \tag{5.8}$$

in agreement with (4.45) for nearest-neighbor step repulsions; g_3 is given in terms of $\breve{g}$ below. The step chemical potential μ resulting variationally is local, properly identified with (4.22).

We proceed to derive (5.8) in the spirit of the analysis in [42, 48]. By definition of $E^{\rm int}$ and use of the co-area formula, (4.41), we have

$$\begin{aligned} E^{\rm int} &= \frac{\breve{g}}{2}\sum_i \int_{L_i} \mathrm{d}s\; U_i^{\rm int} \\ &= \frac{\breve{g}}{2a}\int_{\mathcal{R}} \mathrm{d}\mathbf{r}\; |\nabla h| \lim_{\epsilon\to 0}\sum_{j=1}^{\infty}[\tilde{\Phi}(\eta_i,\eta_{i+j})m_{i,i+j}^2 + \tilde{\Phi}(\eta_i,\eta_{i-j})m_{i,i-j}^2]. \end{aligned} \tag{5.9}$$

In order to determine the limit of $m_{i,i\pm j}$ as $\epsilon\to 0$ we view the local variable η_i as a continuous and sufficiently differentiable function $\eta(h,t)$ of the height h; this function results from inverting the relation $h|_{\eta=\eta_i} - h|_{\eta=\eta_{i+1}} = a$. Consequently, using $\zeta=\zeta(h,t)$ via suppressing the dependence on σ, we obtain

$$\lim_{\epsilon\to 0} m_{i,i\pm j} = \frac{1}{j\,\lambda}\left[\lim_{a\to 0}\frac{|\zeta(h\pm ja,t)-\zeta(h,t)|}{ja}\right]^{-1} = \frac{1}{\lambda j}\frac{1}{|\partial_h\zeta|} = \frac{1}{\lambda j}|\partial_\zeta h|, \tag{5.10}$$

where $|\partial_\zeta h| = \lambda|\nabla h|$. Then, (5.9) reduces to

$$E^{\rm int} = \frac{1}{2}\frac{\breve{g}}{a}\int_{\mathcal{R}} \mathrm{d}\mathbf{r}\; |\nabla h|^3 \lim_{\epsilon\to 0}\sum_{j=1}^{\infty}\frac{1}{j^2}[\tilde{\Phi}(\eta_i,\eta_{i+j}) + \tilde{\Phi}(\eta_i,\eta_{i-j})]. \tag{5.11}$$

By assuming that the geometrical factor $\tilde{\Phi}$ is bounded, we infer that the sum over j converges absolutely. Applying homogeneity of the elastic medium and fields we set

$$\tilde{\Phi}_0 \equiv \frac{3}{2}\lim_{\epsilon\to 0}\sum_{j=1}^{\infty}\frac{1}{j^2}[\tilde{\Phi}(\eta_i,\eta_{i+j}) + \tilde{\Phi}(\eta_i,\eta_{i-j})], \tag{5.12}$$

an η-independent function; the factor $3/2$ is included for the sake of direct comparisons with (4.40). Thus, (5.11) yields

$$E^{\rm int} = \frac{1}{3}\frac{\breve{g}\tilde{\Phi}_0}{a}\int_{\mathcal{R}} \mathrm{d}\mathbf{r}\; |\nabla h|^3, \tag{5.13}$$

which is identified with (5.8) if the effective step interaction parameter g_3 is defined by $g_3 = \breve{g}\tilde{\Phi}_0/a$, by analogy with (4.40) for nearest-neighbor step interactions.

We conclude this subsection by discussing more generally conditions on the step interactions that can give rise to local continuum evolution laws. Evidently, the replacement of $m_{i,k}^2$ for each step pair in (5.6) by the general power law $m_{i,k}^\alpha$ preserves the local character of the continuum if $\alpha>1$. In principle, this locality is retained if the summand in (5.6) is replaced by $\mathcal{V}(m_{i,k},\eta_i,\eta_k)$ where $\mathcal{V}(bm,\eta,\nu) = b^\alpha\mathcal{V}(m,\eta,\nu)$ and $\alpha>1$ for any $b>0$, i.e., $\mathcal{V}$ is a homogeneous function of m with degree $\alpha>1$.

5.2. Orientation-dependent step energies. In this subsection we extend the analysis of Sec. 5.1.1 to energies dependent on the step normal angle θ, formed by the local tangent and the y axis; cf. Fig. 3.1. By (3.13), (3.15) and (5.1) we define

$$\gamma=\gamma(\theta),\quad U_i^{\rm int} = g[V(m_i,\zeta_i,\zeta_{i+1},\theta_i) + V(m_i,\zeta_i,\zeta_{i-1},\theta_i)],\quad \theta_i=\theta(\eta_i,\sigma), \tag{5.14}$$

where γ is the step line tension, the energy per unit length of an isolated step. This consideration affects only the formula for μ_i. We show that in the continuum limit

$$\mu(\mathbf{r},t) = \frac{\Omega}{a}\nabla\cdot[\partial_m(m\tilde{U}_0)\mathbf{e}_\eta - (\partial_\theta\tilde{U}_0)\mathbf{e}_\sigma], \tag{5.15}$$

where $\tilde{U}_0(m,\theta) \equiv \gamma(\theta) + gV(m,\zeta,\zeta,\theta)$, $\mathbf{e}_\eta$ is given by (4.5) and $\mathbf{e}_\sigma$ is given by (B.2) of Appendix B. In the special case where the interaction term V is independent of θ, μ becomes

$$\mu = \frac{\Omega}{a}\left\{(\gamma+\partial_\theta^2\gamma)\kappa - g\nabla\cdot\left[\partial_m(mV_0)\frac{\nabla h}{|\nabla h|}\right]\right\}, \tag{5.16}$$

where $V_0(m) \equiv V(m,\zeta,\zeta)$, and $\gamma+\partial_\theta^2\gamma$ is known as the "step stiffness" ([1, 44]) and expresses the inertia of the step in the presence of driving forces; compare to (5.2).

We proceed to derive (5.15) and (5.16) by applying the variational formulation of Sec. 4.5.1. The energy of an arbitrary step train is

$$E^{\text{steps}} = \sum_i \int_{L_i} \mathrm{d}s\ [\gamma(\theta_i) + gV(m_i,\zeta_i,\zeta_{i+1},\theta_i)] \to a^{-1}\int\!\!\int \mathrm{d}\mathbf{r}\ |\nabla h|\ \tilde{U}_0(m,\theta). \tag{5.17}$$

By (C.2) of Appendix C and integration by parts, the first variation of E^{steps} reads

$$\dot{E}^{\text{steps}} = a^{-1}\int\!\!\int \mathrm{d}\mathbf{r}\ \nabla\cdot[\partial_m(m\tilde{U}_0)\,\mathbf{e}_\eta - (\partial_\theta\tilde{U}_0)\mathbf{e}_\sigma]\,\partial_t h. \tag{5.18}$$

The comparison of this formula with the variational definition (4.47) for μ yields (5.15).

To derive (5.16) we replace $\tilde{U}_0 = \gamma(\theta) + gV_0(m)$ in (5.15) and use (C.4) and (C.5) of Appendix C:

$$\begin{aligned}\mu &= \frac{\Omega}{a}\nabla\cdot\{[\gamma(\theta)+g\partial_m(mV_0)]\mathbf{e}_\eta - (\partial_\theta\gamma)\mathbf{e}_\sigma\}\\ &= \frac{\Omega}{a}\{\gamma\nabla\cdot\mathbf{e}_\eta - (\partial_\theta^2\gamma)\nabla\theta\cdot\mathbf{e}_\sigma + (\nabla\theta\cdot\mathbf{e}_\eta - \nabla\cdot\mathbf{e}_\sigma)\partial_\theta\gamma + g\nabla\cdot[\partial_m(mV_0)\mathbf{e}_\eta]\},\end{aligned} \tag{5.19}$$

where $\nabla\cdot\mathbf{e}_\eta = \kappa = -\nabla\theta\cdot\mathbf{e}_\sigma$ and $\nabla\theta\cdot\mathbf{e}_\eta = \nabla\cdot\mathbf{e}_\sigma$. Thus, (5.16) is readily obtained. We note in passing that the interaction-related term $\nabla\cdot[\partial_m(mV_0)\mathbf{e}_\eta]$ can be further expanded by use of (C.11) and (C.12) of Appendix C.

6. Conclusion. The continuum limit of a (2+1)-dimensional step flow model was studied systematically in the absence of material deposition, when the stepped surface relaxes to become flat. The effects considered here were isotropic adatom diffusion on each terrace, atom attachment-detachment at each step edge, and pairwise step interactions. Continuum formulas for the step chemical potential and the step velocity were derived from the BCF approach ([3]) and, alternatively, within continuum thermodynamics via a surface free energy, with identical results; cf. Sec. 4.5. By contrast, the relation between surface current and the gradient of step chemical potential, (4.8) with (4.10), requires consideration of the equations for step motion; it can only be determined by coarse graining of BCF-type models and cannot be guessed from one-dimensional models. As a consequence of the coarse graining and the boundary conditions imposed at step edges in 2+1 dimensions, the continuum-scale, vector-valued surface current is related to the gradient of the step chemical potential via a tensor mobility which depends on the surface slope. The corresponding formula

admits a relatively transparent physical interpretation: Transverse adatom fluxes are restricted by attachment-detachment at step edges, whereas longitudinal fluxes are produced by adatoms that hop freely on terraces. The combination of macroscopic evolution laws for the adatom current, step chemical potential and step velocity resulted in a nonlinear, fourth-order PDE for the surface height profile. This equation offers a previously unnoticed interplay of step energetics, step kinetics, and aspect ratio of surface topography.

There are other aspects of surface morphological evolution that were not addressed by our analysis. For example, we have not included material deposition on the surface from above; this effect is studied elsewhere ([31]). Our assumption of a step train with slowly varying step edge curvature poses a considerable limitation. Situations where our formulation is questionable include surface regions where the step radius of curvature exhibits abrupt spatial variations, such as those observed in sputter rippling experiments ([12]). In addition, we neglected bulk stress, which may in principle induce long-range, pairwise attractive or other step interactions ([25, 26]), and lead to non-local evolution laws that may form a (2+1)-dimensional analogue of the integro-differential equation derived in [48]; these matters are left for future work. Our method of coarse graining does not resolve the issue of boundary conditions at facet edges, where continuum solutions become singular and the motion of extremal steps must be taken into account ([5, 21, 15]). The derivation and implementation of the related boundary conditions from step models is work in progress. Germane is the problem of an appropriate numerical treatment of the derived evolution equations for the height profile, which is beyond the scope of this article. Finally, we have not attempted here to provide connections of our theory, in particular of PDE (4.39), with available experimental observations. A plausible connection of this theory to relaxation experiments of bi-periodic profiles is discussed elsewhere ([29]). Our understanding of the initial conditions within continuum that can give rise to observable surface corrugations below T_{R} is currently incomplete. It is hoped that our work will stimulate further studies in this or other directions.

Acknowledgments. We thank Michael J. Aziz, Russel E. Caflisch, Theodore L. Einstein, Robert V. Kukta, Vivek B. Shenoy, Timothy Stasevich, and Howard A. Stone for useful discussions.

Appendix A. Property of nearest-neighbor interaction energy. In this appendix we derive a property of the step interaction term $V_{i,i+1}$ introduced in (3.15), as a direct consequence of condition (3.21). We start with the general formula (5.1), $V_{i,i+1} = V(m_i, \zeta_i, \zeta_{i+1})$, assuming that V does not depend on the step orientation; in the end we extend our results to step orientation dependent V.

First, by (3.21) we impose the condition

$$V(m, \zeta_i, \zeta_{i+1})\, \mathrm{d}s_i = V(m, \zeta_{i+1}, \zeta_i)\, \mathrm{d}s_{i+1} \qquad \forall\ i, \tag{A.1}$$

where $\mathrm{d}s_i = \xi_\sigma|_i\, \mathrm{d}\sigma$ is a properly short length of the ith step edge. Equation (A.1) applies to any pair of step edge contours, each defined by $\mathbf{r}(\eta, \sigma, t)$ with η =const., thus eliminating i and replacing ζ_i by the continuous variable ζ introduced by (3.17) and (3.20) (cf. Fig. 3.1),

$$V(m, \zeta, \chi)\, \mathrm{d}s_{(\zeta)} = V(m, \chi, \zeta)\, \mathrm{d}s_{(\chi)}, \tag{A.2}$$

where $\mathrm{d}s_{(\zeta)}$ is a short length of the step edge associated with ζ. We also define the

one-variable, ζ-independent, function V_0 by

$$V_0(m) = V(m, \zeta, \zeta). \tag{A.3}$$

Second, we prove the following lemma.

LEMMA A.1. *If $V(m, \zeta, \chi)$ is continuously differentiable with (ζ, χ) $\forall$ $m > 0$ then, by (A.3),*

$$\partial_\zeta V(m, \zeta, \chi) = -\partial_\zeta V(m, \chi, \zeta) \qquad \zeta = \chi. \tag{A.4}$$

Proof. For fixed step density m and $(\zeta, \chi) \to (\tilde{\rho}, \tilde{\rho})$, $V(m, \zeta, \chi)$ has the expansion

$$V(m, \zeta, \chi) \sim V_0(m) + \partial_\zeta V(\zeta, \tilde{\rho})|_{\tilde{\rho}}\,(\zeta - \tilde{\rho}) + \partial_\chi V(\tilde{\rho}, \chi)|_{\tilde{\rho}}\,(\chi - \tilde{\rho}). \tag{A.5}$$

Then, (A.4) follows by allowing $\zeta = \chi$ in (A.5). This statement concludes the proof. (Alternatively, one can differentiate both sides of (A.3) with respect to ζ.) ∎

Next, we prove a proposition needed for the continuum limit of Sec. 4.2.

PROPOSITION A.2. *If $V(m, \zeta, \chi)$ is continuously differentiable with (ζ, χ) $\forall$ $m > 0$ and satisfies (A.2) and (A.3), then*

$$\partial_\zeta V(m, \zeta, \chi) = -\frac{\lambda\kappa}{2}\, V_0(m), \qquad \zeta = \chi, \tag{A.6}$$

where λ is the macroscopic length of (3.20), and κ is the curvature of the contour $\eta = c$=const.; for given $\zeta = \chi$, the c is defined by (3.17) with $\eta = c$ and $\rho = \lambda\,\zeta$.

Proof. We start with (A.1) for notational convenience, where $\mathrm{d}s_{i+1} = \xi_\sigma|_{i+1}\,\mathrm{d}\sigma$, by considering $\delta\zeta_i = \zeta_{i+1} - \zeta_i \to 0$. By using the expansions

$$V(m, \zeta_i, \zeta_{i+1}) \sim V_0(m) + \delta\zeta_i\, \partial_\zeta V(m, \zeta_i, \zeta)|_{\zeta_i}, \tag{A.7}$$

$$V(m, \zeta_{i+1}, \zeta_i) \sim V_0(m) + \delta\zeta_i\, \partial_\zeta V(m, \zeta, \zeta_i)|_{\zeta_i}, \tag{A.8}$$

$$\xi_\sigma|_{i+1} \sim \xi_\sigma|_i + \delta\zeta_i\, \partial_{\zeta_i}\xi_\sigma|_i, \tag{A.9}$$

along with $\partial_\eta \xi_\sigma = \kappa \xi_\sigma \xi_\eta$ from (3.11), we reduce (A.1) to

$$\partial_\zeta V(m, \zeta_i, \zeta) - \partial_\zeta V(m, \zeta, \zeta_i) = \lambda\kappa\, V_0(m), \qquad \eta = \eta_i\ (\zeta = \zeta_i). \tag{A.10}$$

The use of Lemma A.1 then yields

$$\partial_\zeta V(m, \zeta, \zeta_i) = -\frac{\lambda\kappa}{2}\, V_0(m), \qquad \zeta = \zeta_i. \tag{A.11}$$

The desired relation (A.6) follows via replacement of ζ_i by the continuous variable ζ via (A.2). This statement concludes the proof. ∎

Next, we address for completeness the case with step-step interactions depending on the step orientation, $V_{i,i+1} = V(m_i, \zeta_i, \zeta_{i+1}, \mathbf{e}_\sigma|_i)$. By analogy with Proposition A.2 we state the following proposition.

PROPOSITION A.3. *If $V(m, \zeta, \chi, \mathbf{e}_\sigma)$ is continuously differentiable with $(\zeta, \chi, \mathbf{e}_\sigma)$ $\forall$ $m > 0$ and satisfies*

$$V(m, \zeta_i, \zeta_{i+1}, \mathbf{e}_\sigma|_i)\,\mathrm{d}s_i = V(m, \zeta_{i+1}, \zeta_i, \mathbf{e}_\sigma|_{i+1})\,\mathrm{d}s_{i+1} \qquad \forall\ i, \tag{A.12}$$

and $V(m,\zeta,\zeta,\mathbf{e}_\sigma) \equiv V_0(m,\mathbf{e}_\sigma)$*, then*

$$\partial_\zeta V(m,\zeta,\chi,\mathbf{e}_\sigma) = -\frac{\lambda\kappa}{2}\,V_0(m,\mathbf{e}_\sigma) - \frac{1}{2}\nabla_{\mathbf{e}_\eta} V(m,\zeta,\chi,\mathbf{e}_\sigma)\cdot\partial_\zeta \mathbf{e}_\sigma \qquad \zeta=\chi. \tag{A.13}$$

Proof. Because the proof is similar to that for Proposition A.2, we omit most of the details here. We only note the more general expansion

$$\begin{aligned} V(m,\zeta_{i+1},\zeta_i,\mathbf{e}_\sigma|_{i+1}) \sim V_0(m,\mathbf{e}_\sigma|_i) + \delta\zeta_i[\partial_\zeta V(m,\zeta,\zeta_i,\mathbf{e}_\sigma|_i) \\ + \nabla_{\mathbf{e}_\eta} V(m,\zeta_i,\zeta_i,\mathbf{e}_\sigma)\cdot\partial_{\tilde\rho_i}\mathbf{e}_\sigma] \end{aligned} \tag{A.14}$$

in place of (A.8), in order to account for the dependence on $\mathbf{e}_\sigma$. Equation (A.13) follows by direct analogy with (A.7)–(A.10). ∎

Appendix B. Cartesian representation of mobility tensor. In this appendix we derive (4.21), the representation of the mobility tensor (4.10) in the Cartesian coordinates (x,y) of the basal plane, in the form of the following proposition.

PROPOSITION B.1. *If the continuum-scale surface height profile* $h(\mathbf{r},t)$ *is* $\mathbf{r}$*-differentiable and* $\nabla h \neq 0$*, the mobility tensor,* $\mathbf{M} = \frac{D_s}{k_B T}\,\mathbf{\Lambda}$*, in the basal plane's Cartesian system* $(x,\,y)$*, where* $\nabla = (\partial_x\ \partial_y)^{\mathrm{T}}$*, is represented via the* 2×2 *matrix*

$$\mathbf{\Lambda} = \begin{pmatrix} \dfrac{1}{1+q\,|\nabla h|}\dfrac{(\partial_x h)^2}{|\nabla h|^2} + \dfrac{(\partial_y h)^2}{|\nabla h|^2} & -\dfrac{q|\nabla h|}{1+q|\nabla h|}\dfrac{(\partial_x h)\,(\partial_y h)}{|\nabla h|^2} \\ -\dfrac{q|\nabla h|}{1+q|\nabla h|}\dfrac{(\partial_x h)\,(\partial_y h)}{|\nabla h|^2} & \dfrac{1}{1+q|\nabla h|}\dfrac{(\partial_y h)^2}{|\nabla h|^2} + \dfrac{(\partial_x h)^2}{|\nabla h|^2} \end{pmatrix}. \tag{B.1}$$

Proof. First, we describe the continuum-scale unit vector $\mathbf{e}_\sigma$, which is parallel to step edges, in terms of the height profile $h(\mathbf{r},t)$. If $\mathbf{e}_z$ is the unit vector normal to the basal plane, then by (4.5)

$$\mathbf{e}_\sigma = \mathbf{e}_z \times \mathbf{e}_\eta = -\mathbf{e}_z \times \frac{\nabla h}{|\nabla h|} = \frac{(\partial_y h\ \ -\partial_x h)^{\mathrm{T}}}{|\nabla h|}, \tag{B.2}$$

where for the purposes of this appendix all vector-valued quantities are considered column vectors; $\mathbf{U}^{\mathrm{T}}$ denotes the transpose of $\mathbf{U}$. The continuum-scale unit vector $\mathbf{e}_\eta$, which is normal to step edges, is given in terms of ∇h by (4.5).

Second, we seek an expression for $\mathbf{M}$ in Cartesian coordinates as a matrix product. For this purpose we introduce the non-singular matrix

$$\boldsymbol{\mathcal{S}} = (\mathbf{e}_\eta\ \mathbf{e}_\sigma) = \begin{pmatrix} -\dfrac{\partial_x h}{|\nabla h|} & \dfrac{\partial_y h}{|\nabla h|} \\ -\dfrac{\partial_y h}{|\nabla h|} & -\dfrac{\partial_x h}{|\nabla h|} \end{pmatrix}, \qquad \det\boldsymbol{\mathcal{S}} = 1, \tag{B.3}$$

which transforms the local, (η,σ)-representation, $\mathbf{V}_{(\eta,\sigma)} = (V_\eta\ V_\sigma)^{\mathrm{T}}$, of a column vector $\mathbf{V}$ to its Cartesian, (x,y)-representation, $\mathbf{V}_{(x,y)} = (V_x\ V_y)^{\mathrm{T}}$ by

$$\mathbf{V}_{(x,y)} = \boldsymbol{\mathcal{S}}\cdot\mathbf{V}_{(\eta,\sigma)}. \tag{B.4}$$

By applying (B.4) to the vectors $\mathbf{J}$ and $\nabla\mu$ of relation (4.8), $\mathbf{J} = -C_s\mathbf{M}\nabla\mu$, we have

$$\mathbf{J}_{(x,y)} \equiv \begin{pmatrix} J_x \\ J_y \end{pmatrix} = -C_s\,\boldsymbol{\mathcal{S}}\mathbf{M}_{(\eta,\sigma)}\boldsymbol{\mathcal{S}}^{-1}\,\nabla_{x,y}\mu, \tag{B.5}$$

where $\mathbf{M}_{(\eta,\sigma)}$ is the (η,σ)-representation of $\mathbf{M}$, given by (4.10), $\nabla_{(x,y)} = (\partial_x\ \partial_y)^{\mathrm{T}}$, and by (B.3)

$$\boldsymbol{\mathcal{S}}^{-1} = \begin{pmatrix} -\dfrac{\partial_x h}{|\nabla h|} & -\dfrac{\partial_y h}{|\nabla h|} \\ \dfrac{\partial_y h}{|\nabla h|} & -\dfrac{\partial_x h}{|\nabla h|} \end{pmatrix}. \tag{B.6}$$

Hence, the Cartesian representation, $\mathbf{M}_{(x,y)}$, of $\mathbf{M}$ is described via

$$\boldsymbol{\Lambda}_{(x,y)} = \begin{pmatrix} -\dfrac{\partial_x h}{|\nabla h|} & \dfrac{\partial_y h}{|\nabla h|} \\ -\dfrac{\partial_y h}{|\nabla h|} & -\dfrac{\partial_x h}{|\nabla h|} \end{pmatrix} \begin{pmatrix} \dfrac{1}{1+q\,|\nabla h|} & 0 \\ 0 & 1 \end{pmatrix} \begin{pmatrix} -\dfrac{\partial_x h}{|\nabla h|} & -\dfrac{\partial_y h}{|\nabla h|} \\ \dfrac{\partial_y h}{|\nabla h|} & -\dfrac{\partial_x h}{|\nabla h|} \end{pmatrix}, \tag{B.7}$$

which yields (B.1) by matrix multiplication. ∎

Appendix C. Identities for surface slope and step normal angle. In this appendix we provide geometric relations for the step density $m = |\nabla h|$ and the normal angle θ, the angle of the local tangent to a step edge with the y axis; cf. Fig. 3.1. These relations are used in the derivation of the continuum step chemical potential in Sec. 5.2. We simplify notation by using $h_x = \partial_x h$ and $h_y = \partial_y h$; θ, $\mathbf{e}_\eta$ and $\mathbf{e}_\sigma$ are

$$\tan\theta = -\frac{h_y}{h_x}, \quad \mathbf{e}_\eta = -\frac{(h_x, h_y)}{|\nabla h|}, \quad \mathbf{e}_\sigma = \frac{(h_y, -h_x)}{|\nabla h|}. \tag{C.1}$$

We state and prove three relevant propositions.

PROPOSITION C.1. *The first variation of the normal angle, θ, is given by*

$$\dot\theta = m^{-1}\,\mathbf{e}_\sigma \cdot \nabla \dot h. \tag{C.2}$$

Proof. From the first of relations (C.1) we have

$$\dot\theta = \left[-\frac{\dot h_y}{h_x} + h_y\,\frac{\dot h_x}{(h_x)^2}\right]\cos^2\theta = \left[-\frac{\dot h_y}{h_x} + h_y\,\frac{\dot h_x}{(h_x)^2}\right]\frac{(h_x)^2}{|\nabla h|^2} = \frac{(h_y, -h_x)}{|\nabla h|^2}\cdot\nabla\dot h, \tag{C.3}$$

by which (C.2) follows via formula (C.1) for $\mathbf{e}_\sigma$. ∎

PROPOSITION C.2. *The gradient, $\nabla\theta$, of the normal angle θ satisfies*

$$\nabla\theta\cdot\mathbf{e}_\eta = \nabla\cdot\mathbf{e}_\sigma, \tag{C.4}$$

$$\nabla\theta\cdot\mathbf{e}_\sigma = -\kappa, \tag{C.5}$$

where κ is the step edge curvature.

Proof. We first show (C.4) directly. The left side is written in the Eulerian coordinates (x, y, h) by differentiating the first of relations (C.1),

$$\nabla\theta = -\frac{(h_x)^2}{|\nabla h|^2}\left(\partial_x\frac{h_y}{h_x}, \partial_y\frac{h_y}{h_x}\right) = \frac{(-h_x h_{xy} + h_y h_{xx}, -h_x h_{yy} + h_y h_{xy})}{|\nabla h|^2}, \tag{C.6}$$

$$\nabla\theta\cdot\mathbf{e}_\eta = \frac{[(h_x)^2 - (h_y)^2]h_{xy} - h_x h_y(h_{xx} - h_{yy})}{|\nabla h|^3}, \tag{C.7}$$

by recourse to formula (C.1) for $\mathbf{e}_\eta$. The right side of (C.4) equals

$$\nabla \cdot \mathbf{e}_\sigma = \partial_x \frac{h_y}{|\nabla h|} - \partial_y \frac{h_x}{|\nabla h|} = \frac{(h_x)^2 h_{xy} + h_x h_y h_{yy} - h_x h_y h_{xx} - (h_y)^2 h_{xy}}{|\nabla h|^3}. \tag{C.8}$$

The comparison of (C.7) and (C.8) yields (C.4).

We next show (C.5) similarly. From (C.1) and (C.6),

$$\begin{aligned} \mathbf{e}_\sigma \cdot \nabla\theta &= \frac{(h_y, -h_x)}{|\nabla h|} \cdot \frac{(-h_x h_{xy} + h_y h_{xx}, -h_x h_{yy} + h_y h_{xy})}{|\nabla h|^2} \\ &= \frac{(h_x)^2 h_{yy} + (h_y)^2 h_{xx} - 2h_x h_y h_{xy}}{|\nabla h|^3}, \end{aligned} \tag{C.9}$$

$$\kappa = \nabla \cdot \mathbf{e}_\eta = -\partial_x \frac{h_x}{|\nabla h|} - \partial_y \frac{h_y}{|\nabla h|} = -\frac{(h_x)^2 h_{yy} + (h_y)^2 h_{xx} - 2h_x h_y h_{xy}}{|\nabla h|^3}. \tag{C.10}$$

Thus, (C.5) readily follows. The proof is complete. ∎

PROPOSITION C.3. *The positive surface slope (step density), $m = |\nabla h|$, satisfies*

$$\nabla m \cdot \mathbf{e}_\eta = -\left(\kappa + \frac{\Delta h}{|\nabla h|}\right), \tag{C.11}$$

$$\nabla m \cdot \mathbf{e}_\sigma = -m \nabla \cdot \mathbf{e}_\sigma. \tag{C.12}$$

Proof. We show (C.11) directly. The left side reads

$$\begin{aligned} \nabla m \cdot \mathbf{e}_\eta &= \left(\frac{h_x h_{xx} + h_y h_{xy}}{|\nabla h|}, \frac{h_x h_{xy} + h_y h_{yy}}{|\nabla h|}\right) \cdot \frac{(-h_x, -h_y)}{|\nabla h|} \\ &= -\frac{(h_x)^2 h_{xx} + (h_y)^2 h_{yy} + 2h_x h_y h_{xy}}{|\nabla h|^2}. \end{aligned} \tag{C.13}$$

Then, (C.11) follows by comparison with formula (C.10). We prove (C.12) by invoking

$$\begin{aligned} \nabla m \cdot \mathbf{e}_\sigma &= \left(\frac{h_x h_{xx} + h_y h_{xy}}{|\nabla h|}, \frac{h_x h_{xy} + h_y h_{yy}}{|\nabla h|}\right) \cdot \frac{(h_y, -h_x)}{|\nabla h|} \\ &= \frac{h_x h_y (h_{xx} - h_{yy}) - [(h_x)^2 - (h_y)^2] h_{xy}}{|\nabla h|^2}, \end{aligned} \tag{C.14}$$

which equals $-|\nabla h| \nabla \cdot \mathbf{e}_\sigma$ by (C.8). ∎

REFERENCES

[1] Y. AKUTSU AND N. AKUTSU, *Relationship between the anisotropic interface tension, the scaled interface width and the equilibrium shape in two dimensions*, J. Phys. A: Math. Gen., 19 (1986), pp. 2813–2820.

[2] L. BALYKOV AND A. VOIGT, *Kinetic model for step flow growth of [100] steps*, Phys. Rev. E, 72 (2005), pp. 022601-1–022601-4.

[3] W. K. BURTON, N. CABRERA, AND F. C. FRANK, *The growth of crystals and the equilibrium structure of their surfaces*, Philos. Trans. R. Soc. London Ser. A, 243 (1951), pp. 299–358.

[4] R. E. Caflisch, W. E, M. F. Gyure, B. Merriman, and C. Ratch, *Kinetic model for a step edge in epitaxial growth*, Phys. Rev. E, 59 (1999), pp. 6879–6887.
[5] A. Chame, S. Rousset, H. P. Bonzel, and J. Villain, *Slow dynamics of stepped surfaces*, Bulgarian Chem. Commun., 29 (1996/97), pp. 398–434.
[6] W. L. Chan, A. Ramasubramaniam, V. B. Shenoy, and E. Chason, *Relaxation kinetics of nano-ripples on Cu(001) surface*, Phys. Rev. B, 70 (2004), pp. 245403-1–245403-9.
[7] G. Danker, O. Pierre-Louis, K. Kassner, and C. Misbah, *Peculiar effects of anisotropic diffusion on dynamics of vicinal surfaces*, Phys. Rev. Lett., 93 (2004), pp. 185504-1–185504-4.
[8] C. Duport, P. Politi, and J. Villain, *Growth instabilities induced by elasticity in a vicinal surface*, J. Phys. I, 5 (1995), pp. 1317–1350.
[9] W. E and N. K. Yip, *Continuum theory of epitaxial growth. I*, J. Stat. Phys., 104 (2001), pp. 221–253.
[10] G. Ehrlich and F. Hudda, *Atomic view of surface diffusion: Tungsten on tungsten*, J. Chem. Phys., 44 (1966), pp. 1039–1099.
[11] L. P. Eisenhart, *An Introduction to Differential Geometry*, pp. 224–230, Princeton University Press, Princeton, NJ, 1947.
[12] J. Erlebacher, M. J. Aziz, E. Chason, M. B. Sinclair, and J. A. Floro, *Nonclassical smoothening of nanoscale surface corrugations*, Phys. Rev. Lett., 84 (2000), pp. 5800–5803.
[13] J. W. Evans, P. A. Thiel, and M. C. Bartelt, *Morphological evolution during epitaxial thin film growth: Formation of 2D islands and 3D mounds*, Surf. Sci. Reports, 61 (2006), pp. 1–128.
[14] L. C. Evans, *Partial Differential Equations*, pp. 149–154, American Mathematical Society, Providence, RI, 2002.
[15] P.-W. Fok, *Simulation of Axisymmetric Stepped Surfaces with a Facet*, Ph.D. Thesis, Massachusetts Institute of Technology, 2006.
[16] R. Ghez, H. G. Cohen, and J.B. Keller, *The stability of growing or evaporating crystals*, J. Appl. Phys., 73 (1993), pp. 3685–3693.
[17] E. E. Gruber and W. W. Mullins, *On the theory of anisotropy of crystalline surface tension*, J. Phys. Chem. Solids, 28 (1967), pp. 875–887.
[18] J. Hager and H. Spohn, *Self-similar morphology and dynamics of periodic surface profiles below the roughening transition*, Surf. Sci., 324 (1995), pp. 365–372.
[19] C. Herring, *Surface tension as a motivation for sintering*, in The Physics of Powder Metallurgy, W. E. Kingston, ed., McGraw-Hill, New York, 1951, pp. 143–179.
[20] D. T. J. Hurle, ed., *Handbook of Crystal Growth*, North Holland, Amsterdam, 1993.
[21] N. Israeli and D. Kandel, *Profile of a decaying crystalline cone*, Phys. Rev. B, 60 (1999), pp. 5946–5962.
[22] N. Israeli and D. Kandel, *Decay of one-dimensional surface modulations*, Phys. Rev. B, 62 (2000), pp. 13707–13717.
[23] H.-C. Jeong and E. D. Williams, *Steps on surfaces: experiments and theory*, Surf. Sci. Reports, 34 (1999), pp. 171–294.
[24] M. E. Keefe, C. C. Umbach, and J. M. Blakely, *Surface self-diffusion on Si from the evolution of periodic atomic step arrays*, J. Phys. Chem. Solids, 55 (1994), pp. 965–973.
[25] R. V. Kukta and K. Bhattacharya, *A micromechanical model of surface steps*, J. Mech. Phys. Solids, 50 (2002), pp. 615–649.
[26] R. V. Kukta, A. Peralta, and D. Kouris, *Elastic interaction of surface steps: Effect of atomic-scale roughness*, Phys. Rev. Lett., 88 (2002), pp. 186102-1–186102-4.
[27] F. Liu and H. Metiu, *Stability and kinetics of step motion on crystal surfaces*, Phys. Rev. E, 49 (1997), pp. 2601–2616.
[28] V. I. Marchenko and A. Ya. Parshin, *Elastic properties of crystal surfaces*, Sov. Phys. JETP, 52 (1980), pp. 129–131.
[29] D. Margetis, *Unified continuum approach to crystal surface morphological relaxation*, submitted.
[30] D. Margetis, M. J. Aziz, and H. A. Stone, *Continuum approach to self-similarity and scaling in morphological relaxation of a crystal with a facet*, Phys. Rev. B, 71 (2005), pp. 165432-1–165432-21.
[31] D. Margetis and R. V. Kohn, *Continuum theory of material deposition on stepped surfaces in 2+1 dimensions*, in preparation.
[32] T. Michely and J. Krug, *Islands, Mounds and Atoms: Patterns and Processes in Crystal Growth Far From Equilibrium*, Springer-Verlag, 2004.
[33] W. W. Mullins, *Theory of thermal grooving*, J. Appl. Phys., 28 (1957), pp. 333–339.
[34] W. W. Mullins, *Flattening of a nearly plane solid surface due to capillarity*, J. Appl. Phys.,

30 (1959), pp. 77–83.
[35] P. Noziéres, *On the motion of steps on a vicinal surface*, J. Phys. (France), 48 (1987), pp. 1605–1608.
[36] M. Ozdemir and A. Zangwill, *Morphological equilibration of a corrugated crystalline surface*, Phys. Rev. B, 42 (1990), pp. 5013–5024.
[37] A. Pimpinelli and J. Villain, *Physics of Crystal Growth*, Cambridge, UK, 1998; see Chap. 15 for a description of step interactions.
[38] A. Rettori and J. Villain, *Flattening of grooves on a crystal surface: A method of investigation of surface roughness*, J. Phys. (France), 49 (1988), pp. 257–267.
[39] J. S. Rowlinson and B. Widom, *Molecular Theory of Capillarity*, Chap. 2, Clarendon Press, Oxford, 1982.
[40] R. L. Schwoebel and E. J. Shipsey, *Step motion on crystal surfaces*, J. Appl. Phys., 37 (1966), pp. 3682–3686.
[41] V. B. Shenoy, A. Ramasubramaniam, H. Ramanarayan, D. T. Tambe, W-L. Chan, and E. Chason, *Influence of step-edge barriers on the morphological relaxation of nanoscale ripples on crystal surfaces*, Phys. Rev. Lett., 92 (2004), pp. 256101-1–256101-4.
[42] V. B. Shenoy and L. B. Freund, *A continuum description of the energetics and evolution of stepped surfaces in strained nanostructures*, J. Mech. Phys. Solids, 50 (2002), pp. 1817–1841.
[43] H. Spohn, *Surface dynamics below the roughening transition*, J. Phys. I (France), 3 (1993), pp. 69–81.
[44] T. J. Stasevich, H. Gebremariam, T. L. Einstein, M. Giesen, C. Steimer, and H. Ibach, *Low-temperature orientation dependence of step stiffness on {111} surfaces*, Phys. Rev. B, 71 (2005), pp. 245414-1–245414-11.
[45] S. Tanaka, N. C. Bartelt, C. C. Umbach, R. M. Tromp, and J. M. Blakely, *Step permeability and the relaxation of biperiodic gratings on Si(001)*, Phys. Rev. Lett., 78 (1997), pp. 3342–3345.
[46] J. Tersoff, M. D. Johnson, and B. G. Orr, *Adatom densities on GaAs: Evidence for near-equilibrium growth*, Phys. Rev. Lett., 78 (1997), pp. 282–285.
[47] J. Tersoff, Y. H. Phang, Z. Zhang, and M. G. Lagally, *Step-bunching instability of vicinal surfaces under stress*, Phys. Rev. Lett., 75 (1995), pp. 2730–2733.
[48] Y. Xiang, *Derivation of a continuum model for epitaxial growth with elasticity on vicinal surface*, SIAM J. Appl. Math., 63 (2002), pp. 241–258.
[49] Y. Xiang and W. E, *Misfit elastic energy and a continuum model for epitaxial growth with elasticity on vicinal surfaces*, Phys. Rev. B, 69 (2004), pp. 035409-1–035409-15.